

Spatiotemporal Trends in Water Chemistry and Benthic Macroinvertebrates of Headwater Streams Influenced by Surface Coal Mining in Central Appalachia

Powell River Project Annual Report 2018–2019

T.R. Cianciolo, S.H. Schoenholtz, D.L. McLaughlin
Virginia Water Resources Research Center and
Department of Forest Resources and Environmental Conservation
Virginia Tech

August 16, 2019

INTRODUCTION

Increased concentrations of dissolved inorganic salts (i.e., salinity) in freshwater streams is a global problem resulting from various forms of anthropogenic land use, including resource extraction, urbanization, and agriculture (Kaushal et al. 2018). Salinization of streams threatens biodiversity and ecosystem function with additional impacts to human health and infrastructure (Cañedo-Argüelles et al. 2016). For example, anthropogenic salinization of freshwater has been linked to altered fish assemblages (Higgins and Wilde 2005), shifts in macroinvertebrate community structure and trait composition (Szöcs et al. 2014), and reduced reproductive success and survivability in freshwater mussels (Blakeslee et al. 2013; Beggel and Geist 2015). In the central Appalachian coalfield, surface-mining activity is a major contributor to increased salinity in headwater streams (Griffith et al. 2012). Increased loading of dissolved ions in streams draining mined areas is persistent over time (Evans et al. 2014) and distance downstream (Johnson et al. 2019), highlighting the need for long-term study of salinity and associated impacts to biological communities in these systems downstream of mining activities.

In central Appalachia, approximately 3.5% (5,900 km²) of the land area has been impacted from surface mining (Pericak et al. 2018), with documented effects to water chemistry of headwater streams (Palmer et al. 2010). Surface mining activities expose buried coal seams by removing overlying layers of bedrock using explosives and earth-moving equipment (USEPA 2011a). Waste rock, or overburden, is deposited into the adjacent valleys of headwater streams, effectively burying stream channels under tens to hundreds of meters of waste rock (USEPA 2011a). This deposited overburden is exposed to air and water, accelerating natural weathering processes and increasing loading of dissolved ions to headwater streams. In central Appalachia, the acids produced by pyrite oxidation are often buffered by neutralizers released from dissolution of carbonates and other associated minerals, resulting in drainage waters that are often alkaline (Clark et al. 2018a). Resultant alkaline drainage that flows out of impacted areas is enriched in major ions including sulfate (SO₄²⁻), bicarbonate (HCO₃⁻), calcium (Ca²⁺), and magnesium (Mg²⁺) and has elevated pH, total dissolved solids (TDS), and specific conductance (SC) (Pond et al. 2008; Palmer 2010; Timpano et al. 2015).

Numerous studies have documented that elevated salinity, often measured in the field as SC, impacts benthic macroinvertebrate communities in streams draining mined areas in the central Appalachia coalfield (Merricks et al. 2007; Pond et al. 2008; Boehme et al. 2016; Timpano et al. 2015, 2018b). Streams with elevated salinity have reduced taxon richness and community structure shifted to more-tolerant taxa (Pond et al. 2008; Timpano et al. 2018b). Sensitive taxa including *Ephemeroptera* (mayflies) can be absent in streams with high salinity (Merricks et al. 2007). Moreover, the scraper functional feeding group of benthic macroinvertebrates has been documented to have lower richness and abundance in streams with elevated SC compared to reference streams (Pond et al. 2014; Timpano et al. 2018b). Loss of benthic macroinvertebrate taxa and specific functional feeding groups is ecologically important because of their significant role in decomposition and nutrient cycling, as well as being an important food source for higher trophic levels in headwater streams (Wallace and Webster 1996).

Because of their functional role in aquatic ecosystems, benthic macroinvertebrates are useful indicators of water quality conditions and thus stream impairment (Wallace and Webster 1996). The U.S. EPA's Rapid Bioassessment Protocols (RBPs) are used for assessing physical habitat, water quality, and biological stream conditions (Barbour et al. 1999) and rely heavily on a suite of metrics that characterize benthic macroinvertebrate communities. Central Appalachian states commonly use such RBPs and associated evaluations of benthic macroinvertebrate community structure to assess water quality under the Clean Water Act, which regulates water quality in surface mining-influenced streams. Example state-specific RBPs include the Virginia Stream Condition Index (VSCI) and the West Virginia Stream Condition Index (WVSCI) (Burton and Gerritsen 2003; Gerritsen et al. 2000, respectively). Benthic macroinvertebrates are used in such RBPs because they are easy to sample in the field and integrate time-varying water chemistry and habitat conditions (Barbour et al. 1999). Further, benthic macroinvertebrates vary in sensitivity to SC and dissolved ion composition (Barbour et al. 1999) and thus can indicate effects of altered water chemistry from mining impacts. However, improved quantification of associations between measured water chemistry and responses in benthic macroinvertebrate community structure is needed to inform regulatory standards for headwater streams in the central Appalachian region (Timpano et al. 2015; Boehme et al. 2016).

As weathering of mine spoils in closed and reclaimed coal mines continues with time, it is likely that water chemistry in affected headwater streams will change (Clark et al. 2018b) as could its impact on aquatic biota (Pond et al. 2014). Streams that receive discharge from mined areas can be impacted by elevated SC long after termination of mining and restoration activities, with likely sustained effects to benthic macroinvertebrate communities. Evans et al. (2014) monitored SC across a chronosequence of 127 streams that ranged from 1 to 23 years since establishment of valley fills and modelled mean recovery time to attain relatively low TDS levels ($SC < 500 \mu\text{s/cm}$) as 19.6 years after closure of mining and revegetation. Daniels et al. (2016) conducted laboratory leaching tests of mine spoils and found gradual decline of SC over time, but hypothesized recovery time on the scale of decades. Neither Evans et al. (2014) nor Daniels et al. (2016) documented TDS decline to the $< 200 \mu\text{s/cm}$ conditions that characterize relatively undisturbed streams of this region. However, long-term monitoring studies are needed to continuously measure SC over a range of sites in the central Appalachian coalfield to better

understand temporal trends in water chemistry following surface mining activities. Further, to our knowledge, there are few long-term studies of how biotic response may change with time since mining operations (see Pond et al. 2014), highlighting the need for long-term, coupled study of SC and attendant response of benthic macroinvertebrate communities.

The ion matrix that constitutes salinity of surface mining-influenced headwater streams may also vary spatially across the stream network and with flow conditions. Such spatiotemporal variation in water chemistry can be influenced by several processes, including dilution, constituent source activation, and biogeochemical transformations (Zimmer et al. 2013, Tiwari et al. 2017). For example, major ions leached from waste overburden (e.g. SO_4^{2-} , Ca^{2+} , sodium (Na^+), and Mg^{2+}) are largely conservative, with water column concentrations declining with distance downstream in response to inputs of more-dilute groundwater (Johnson et al. 2019). However, other elements, such as iron (Fe) and manganese (Mn), can respond to changing redox conditions (e.g., valley fill pond, wetland establishment). These processes also can vary with differing flow conditions and stream attributes (Temnerud and Bishop 2005), as can different constituent sources (Paybins 2003). Effects of continued weathering can also alter both the ion matrix and the conductivity of leachate waters (Clark et al. 2018b). Consequently, downstream water quality can be highly dynamic over time and across site conditions, highlighting a research need to better understand downstream impacts of surface mining (Johnson et al. 2019).

In this study, we continued to build upon a rich long-term dataset of 30-minute, continuous SC data and seasonal sampling of benthic macroinvertebrates and water chemistry across 23 headwater streams in central Appalachia. Our objectives were to assess long-term temporal trends in SC, ion matrix, and benthic macroinvertebrate community metrics. We also used high spatial-resolution sampling across three of these streams to assess spatial- and flow-driven variability of water chemistry within small-watershed ($< 1.5 \text{ km}^2$) headwater streams influenced by surface mining.

METHODS

Site Selection

The 23 study headwater streams are located in the coalfield region of southwestern VA and southern WV (Figure 1). These streams were identified to meet rigorous criteria for water chemistry and habitat quality and to isolate TDS as a stressor to aquatic life (Table 1; Timpano et al. 2015). Of the 23 study streams, 18 are mining-influenced “test” streams influenced by surface coal mining. The other five are reference streams within relatively undisturbed, forested watersheds. Both reference and test sites have comparable riparian and in-stream habitat conditions and have been selected such that other potential stressors such as excessive sedimentation, channelization, extreme pH, and low dissolved oxygen are minimized within a 100 m sample reach. A subset of three of the 18 test streams was identified for high-resolution spatial sampling of multiple water chemistry constituents (Figure 1). These streams were identified to have land access permission throughout the entire watershed and to have a watershed area $< 1.5 \text{ km}^2$ (Table 2).

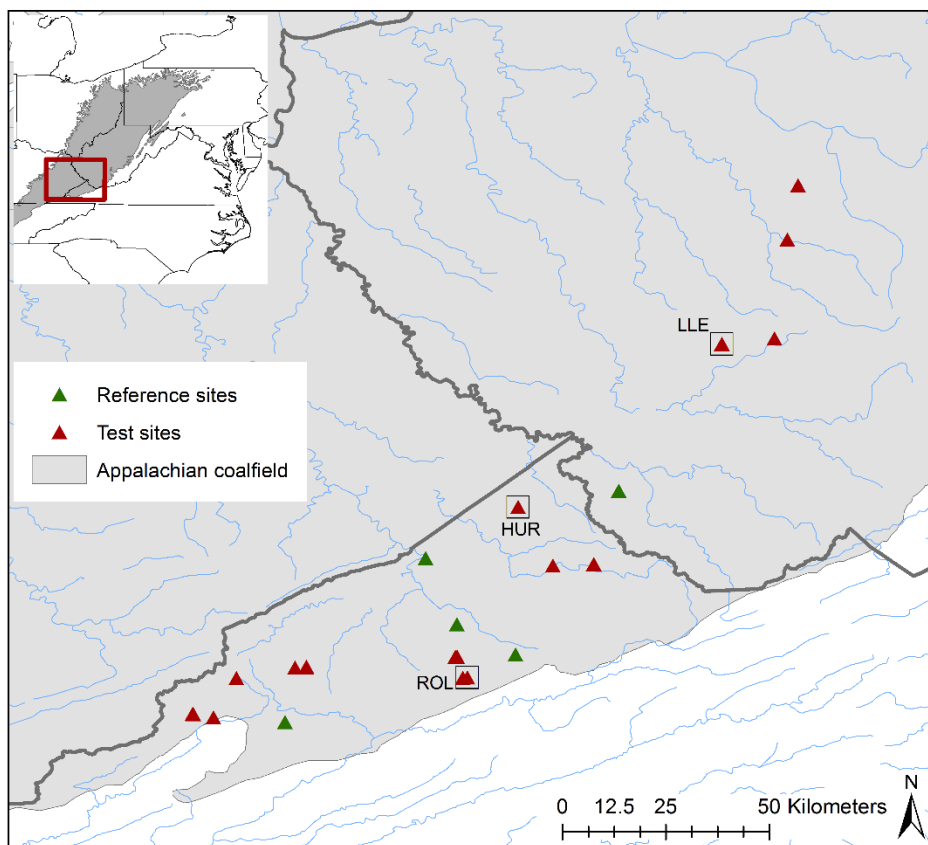


Figure 1: Location of 23 study streams in the coalfield region (shaded gray area) of southern WV and southwestern VA. Five are reference sites (green triangles) and 18 are test sites influenced by surface mining (red triangles). The selected subset of three test streams for high-resolution spatial sampling are within the black square outlines.

Table 1: Abiotic criteria for selection of reference and test streams (Timpano et al. 2015).

| Parameter or condition (units or range) | Selection Criterion ¹ |
|--|----------------------------------|
| Dissolved oxygen (mg/L) | ≥ 6.0 |
| pH | ≥ 6.0 & ≤ 9.0 |
| Epifaunal substrate score (0-20) ² | ≥ 11 |
| Channel alteration score (0-20) ² | ≥ 11 |
| Sediment deposition score (0-20) ² | ≥ 11 |
| Bank disruptive pressure score (0-20) ² | ≥ 11 |
| Riparian vegetation zone width score, per bank (0-10) ² | ≥ 6 |
| Total RBP habitat score (0-200) ² | ≥ 140 |
| Residential land use immediately upstream | none |

¹Parameters and numeric selection criteria from Burton and Gerristen (2003). ²RBP habitat, high gradient streams (Barbour et al. 1999).

Table A: Watershed characteristics for three Appalachian headwater streams selected for high-resolution sampling.

| Site ID | annual mean SC ($\mu\text{s}/\text{cm}$) | watershed area (km ²) | %watershed mined ¹ |
|---------|---|-----------------------------------|----------------------------------|
| LLE | 562 | 0.67 | 11 |
| HUR | 383 | 1.49 | 21 |
| ROL | 625 | 1.33 | 30 |

¹%watershed mined between 1980 and 2016 calculated using a time series of leaf-on clear sky Landsat satellite images and techniques utilized by Li et al. (2015).

Data Collection – Temporal Trends in SC, Ion Matrix, and Benthic Macroinvertebrates

Water Chemistry

In situ SC and stream temperature were measured every 30 minutes from fall 2011 to summer 2019 using automated dataloggers (HOBO Freshwater Conductivity Data Logger, model U24-001, Onset Computer Corp., Bourne, Massachusetts) installed within the 100-m stream reach comprising each study site. Seasonal (i.e., spring and fall) water chemistry monitoring included standard *in situ* measures of water temperature, SC, and pH via a calibrated handheld multi-probe meter (YSI Professional Plus –YSI, Inc., Yellow Springs, Ohio, USA) from fall 2011 to spring 2019.

Seasonal (i.e., spring and fall) grab samples were also collected to assess the ionic composition of streamwater at baseflow (i.e., not during a storm event) from fall 2011 to spring 2019. Water was collected in a clean, plastic bucket below a riffle within the 100-m study reach of each stream where stream water was vertically mixed. Water was drawn into a sterile 60-ml syringe and pushed through a 0.45- μm pore filter into pre-labeled sterile polyethylene water chemistry sample bags. Filtered streamwater was collected in separate 100-ml aliquots for analysis of TDS and alkalinity and in separate 50-ml aliquots for analysis of trace elements/cations and anions. Approximately six drops of 1+1 concentrated ultrapure nitric acid was added to the cation sample to lower the pH below 2 (UESPA 1996). Samples were stored in a cooler on ice and transported to the lab where they were stored at 4 °C until analysis.

Samples were analyzed for TDS by evaporating 50 ml of sample water for test sites and 100 ml of sample water for reference sites in a drying oven at 180 °C (USEPA 1971). Total Alkalinity was measured by titration of a field-filtered water sample with a prepared standard acid using a potentiometric auto-titrator (TitraLab 865, Radiometer Analytical, Lyon, France) (APHA 2005). Calculations of HCO_3^- and CO_3^{2-} were made from Total Alkalinity and pH measurements (APHA 2005). Samples were analyzed for major cations (Ca^{2+} and Mg^{2+}) by ICP-MS. (Thermo iCAP-RQ) (UESPA 1996). An ion chromatograph (Dionex ICS 3000) was used to measure concentrations of chloride (Cl^-) and SO_4^{2-} .

Benthic Macroinvertebrate Community Structure

Benthic macroinvertebrates were sampled in study streams using the semi-quantitative, single habitat (riffle-run) method established by the Virginia Department of Environmental Quality (VDEQ 2008). Approximately six, 1-meter riffles throughout each 100-m study reach were sampled using a 0.3m-wide D-frame kicknet with 500- μ m mesh size to achieve a sample area of 2 m². Sampled riffles were representative of reach hydrology and had sufficient water velocity to wash dislodged benthic macroinvertebrates into the kicknet. A single composite sample was made from the six riffle kicks in each stream and preserved in 95% ethanol. Samples were returned to the lab for sorting and identification.

In the laboratory, composite macroinvertebrate samples were washed with water and cleaned to remove sediment, leaf material, and detritus. Each cleaned sample was evenly spread on a gridded tray for sub-sampling. Semi-quantitative composite samples were sub-sampled following the EPA Rapid Bioassessment Protocol (Barbour et al. 1999), and Virginia Department of Environmental Quality standard operating procedures (VDEQ 2008). Random sub-samples contained a specimen-count of 200 ($\pm 20\%$) individuals and were stored in labeled vials until identification. Sub-sampled individuals were identified to the genus level using standard keys except individuals in family Chironomidae and subclass Oligochaeta, which were identified at those levels.

Data Collection – Spatial Patterns in Water Chemistry

The downstream boundary of the three stream reaches selected for detailed spatial assessment of water chemistry variation was defined as the *in-situ* SC datalogger location used for the long-term study. Each of the three selected streams was sampled twice (Table 3), once after a rain event under highflow conditions and again after a period of no rain under baseflow conditions. During each sampling event, samples were collected every 100 m along the stream mainstem moving up the watershed from the *in-situ* SC datalogger location. When a tributary was reached, samples were taken in the main channel directly above and below the tributary as well within tributary. At each sample location, *in situ* measures of water temperature, SC, and pH were made via a calibrated handheld multi-probe meter (YSI Professional Plus –YSI, Inc., Yellow Springs, Ohio, USA). Grab samples of streamwater were also taken to assess ionic composition. When sufficient stream velocity was present, a water sample was collected in a clean, plastic bucket below a riffle where streamwater had been vertically mixed. Water was then drawn into a sterile 60-ml syringe and pushed through a 0.45- μ m pore filter into pre-labeled sterile polyethylene water chemistry sample bags. When sufficient stream velocity was not present (e.g., at the upper reaches of tributaries), water was drawn from the stream channel directly into a 60-ml sterile syringe. Filtered streamwater was collected in a 100-ml aliquot for analysis of alkalinity and in separate 50-ml aliquots for analysis of trace elements/cations and anions. Approximately six drops of 1+1 concentrated ultrapure nitric acid was added to the cation sample to lower the pH below 2 (UESPA 1996). Samples were stored in a cooler on ice and transported to the lab where they were stored at 4°C until analysis.

Samples were analyzed for Total Alkalinity by titration of a field-filtered water sample with a prepared standard acid using a potentiometric auto-titrator (TitraLab 865, Radiometer Analytical,

Lyon, France) (APHA 2005). Calculations of HCO_3^- and CO_3^{2-} concentrations were made from Total Alkalinity and pH measurements (APHA 2005). Samples were analyzed for major cations (Ca^{2+} , Mg^{2+} , K^+ , Na^+) and dissolved trace elements (B, Al, Cr, Cu, Co, Fe, Ni, Mo, Cd, Ba, Pb, Mn, Se, Zn) by ICP-MS (Thermo iCAP-RQ) (USEPA 1996). An ion chromatograph (Dionex ICS 3000) was used to measure concentrations of Cl^- and SO_4^{2-} .

Table 1: Sampling dates and antecedent precipitation for spatial sampling events at three headwater streams influenced by surface mining.

| Site ID | Date sampled | flow type | 4-day precipitation (in) ¹ |
|---------|--------------|-----------|---------------------------------------|
| ROL | 6/6/2018 | base | 0.08 |
| ROL | 6/27/2018 | high | 1.33 |
| LLE | 12/6/2018 | base | 0.26 |
| LLE | 11/10/2018 | high | 0.93 |
| HUR | 3/14/2019 | base | 0.18 |
| HUR | 11/16/2018 | high | 1.7 |

¹ Data combined from Daily Summary Observations produced by the National Oceanic and Atmospheric Administration (NOAA)

Data Analysis – Temporal Trends in SC, Ion Matrix, and Benthic Macroinvertebrates

To investigate temporal trends in salinity, weekly mean SC values were calculated for all 23 study streams using 30-minute continuous SC data. A modified seasonal Kendall (SK) analysis (Hirsch and Slack 1984) was conducted on these weekly means to assess monotonic temporal trends while accounting for serial dependence and seasonality. This non-parametric analysis is commonly used for water quality time-series data (e.g., Stoddard et al. 1999; Driscoll et al. 2003; Duan et al. 2018) and is resistant to data gaps. The SK test, originally proposed by Hirsch and Slack (1982), conducts an individual Mann-Kendall analysis (Mann 1945) for monotonic trend on each of n seasons separately (e.g., mean SC for week1 is only compared to other week1 mean SC values). An overall Z statistic (S_k) for trend across all seasons is calculated by summing each season's Mann-Kendall statistic (S) (Equation 1).

$$S_k = \sum_{i=1}^n S_i \quad (1)$$

The original SK test estimates the variance of the overall test statistic S_k given by Equation 2 with covariance assumed to be zero because of independence between seasons. The modified SK accounts for serial dependence by estimating the covariance (σ_{ij}) between test statistics given by Equation 3.

$$Var(S_k) = \sum_{i=1}^{n_k} \frac{n_i(n_i-1)(2n_i+5)}{18} \quad (2)$$

$$Var(S_k) = \sum_{i=1}^{n_k} \frac{n_i(n_i-1)(2n_i+5)}{18} + 2 \sum_{i=1}^{n_k-1} \sum_{j=i+1}^{n_k} \sigma_{ij} \quad (3)$$

A Theil-Sen slope analysis (Theil 1950; Sen 1968) was then used to analyze the magnitude of trends when significant, based on the modified SK. The Theil-Sen slope analysis is a nonparametric test that is insensitive to outliers and tests the relationship between two variables (Helsel and Hirsch 2002), in this case SC and time. The output slope is the median value of slopes calculated between all pairs of sample points.

Ionic composition of streamwater was evaluated using both an anion and cation matrix indicator on a millimolar (mmol) basis (Timpano et al. 2017). Ratio of sulfate to bicarbonate ($SO_4:HCO_3$) was chosen as the anion indicator because laboratory studies have shown that sulfate is the dominant anion early in the leaching process of mine spoils and slowly decreases in concentration with repeated leaching events (Orndorff et al. 2015; Daniels et al. 2016). In contrast, concentration of bicarbonate slowly increases with repeated leaching events (Orndorff et al. 2015; Daniels et al. 2016). Ratio of calcium to magnesium (Ca:Mg) was chosen as a cation matrix indicator because previous work has observed reduced Ca:Mg ratio in mining-influenced streams influenced by surface coal mining relative to reference streams (Timpano et al. 2017; Clark et al. 2018a). Differences in these cation and anion matrix indicators between reference and mining-influenced streams were analyzed for site-type effect with study stream defined as a random variable. Temporal trends for each stream were then analyzed using mixed models with ion ratios as the dependent variable and year (numeric) and season (categorical) as independent variables. P-values < 0.05 indicated a significant effect by year and thus a significant temporal trend.

Temporal trends in biological conditions were evaluated using eight metrics describing benthic macroinvertebrate structure (Barbour et al. 1999). Each of the selected metrics has been shown to respond negatively to increasing SC (Timpano et al. 2015, 2018b); they include measures of taxonomic richness, community composition, and functional feeding groups. We first used spearman correlation to validate the negative relationship between salinity and the selected biological metrics. Correlations between SC measured at the time of sampling and biological metrics across all 23 study streams were made each year (fall 2011 to spring 2018) for both fall and spring sampling seasons. We then analyzed temporal trends in biological metrics using mixed models with metrics as the dependent variable and year (numeric) and season (categorical) as independent variables (Timpano et al. 2017). P < 0.05 indicated a significant effect by year, thus a significant temporal trend.

RStudio software (RStudio, Boston, MA) and R version 3.4.1 (R Core Team 2018) were used for all statistical analyses, with a significance level of $\alpha = 0.05$. The “Envstats” package was used for the modified SK test and the “openair” package was used for Theil-Sen slope analysis.

Data Analysis – Spatial Patterns in Water Chemistry

Maps of spatial variation in SC were made for each stream network and each sampling event using ESRI's ArcGIS, GPS coordinates recorded in the field, and mining layers produced by Pericak et al. (2018). Under baseflow and highflow, relative concentrations of major ions and trace elements compared to stream origin concentrations were plotted against distance downstream (Table C-1). Differences in discharge between highflow and baseflow were not directly measured in the field; however, decreased SC can be used as a surrogate for higher flow in these headwater streams (Timpano et al. 2018a). Effect of the highflow event on water chemistry was analyzed by calculating percent difference in constituent concentrations between highflow and baseflow and plotting those differences with distance downstream. Separate graphs were made for major ions and trace elements. These multiple ways of presenting spatial water chemistry illustrated effects of longitudinal trends, tributary inputs, and variable flow conditions on water quality variation in these surface mining-influenced headwater streams.

RESULTS

Temporal Trends in SC, Ion Matrix, and Benthic Macroinvertebrates

Specific Conductance

Across all 23 study streams, we found no streams with increasing trends in SC and 17 streams with no significant trend in SC from fall 2011 to summer 2019 (Appendix A; Table B-1; Figure 2). However, results did show one significant decreasing temporal trend in SC among the five reference streams: $-1.80 \mu\text{s}/\text{cm yr}^{-1}$ (-2.8% annual mean SC yr^{-1}) and five decreasing trends among the 18 mining-influenced streams. The magnitude of temporal change in these five streams was greater than the one reference stream with decreasing SC, ranging from $-22.74 \mu\text{s}/\text{cm yr}^{-1}$ (-1.9% annual mean SC yr^{-1}) to $-10.57 \mu\text{s}/\text{cm yr}^{-1}$ (-3.7% annual mean SC yr^{-1}).

Ion Matrix

Ratios of $\text{SO}_4:\text{HCO}_3$ were higher in mining-influenced streams (1.75 ± 0.08 SE) than reference streams (0.37 ± 0.03 SE) ($p = 0.026$) (Figure 3). The Ca:Mg ratio was higher in reference streams (1.60 ± 0.07 SE) than mining-influenced streams (1.09 ± 0.02 SE) ($p = 0.028$). Mixed models with year (numeric) and season (categorical) as independent variables resulted in ten of the 18 mining-influenced streams with significant decreasing trends in the $\text{SO}_4:\text{HCO}_3$ ratio (Table B-1), whereas there were no significant trends in reference sites. Only seven of the 23 study streams (5 mining-influenced, 2 reference) had significant trends in Ca:Mg ratio, all of which were negative.

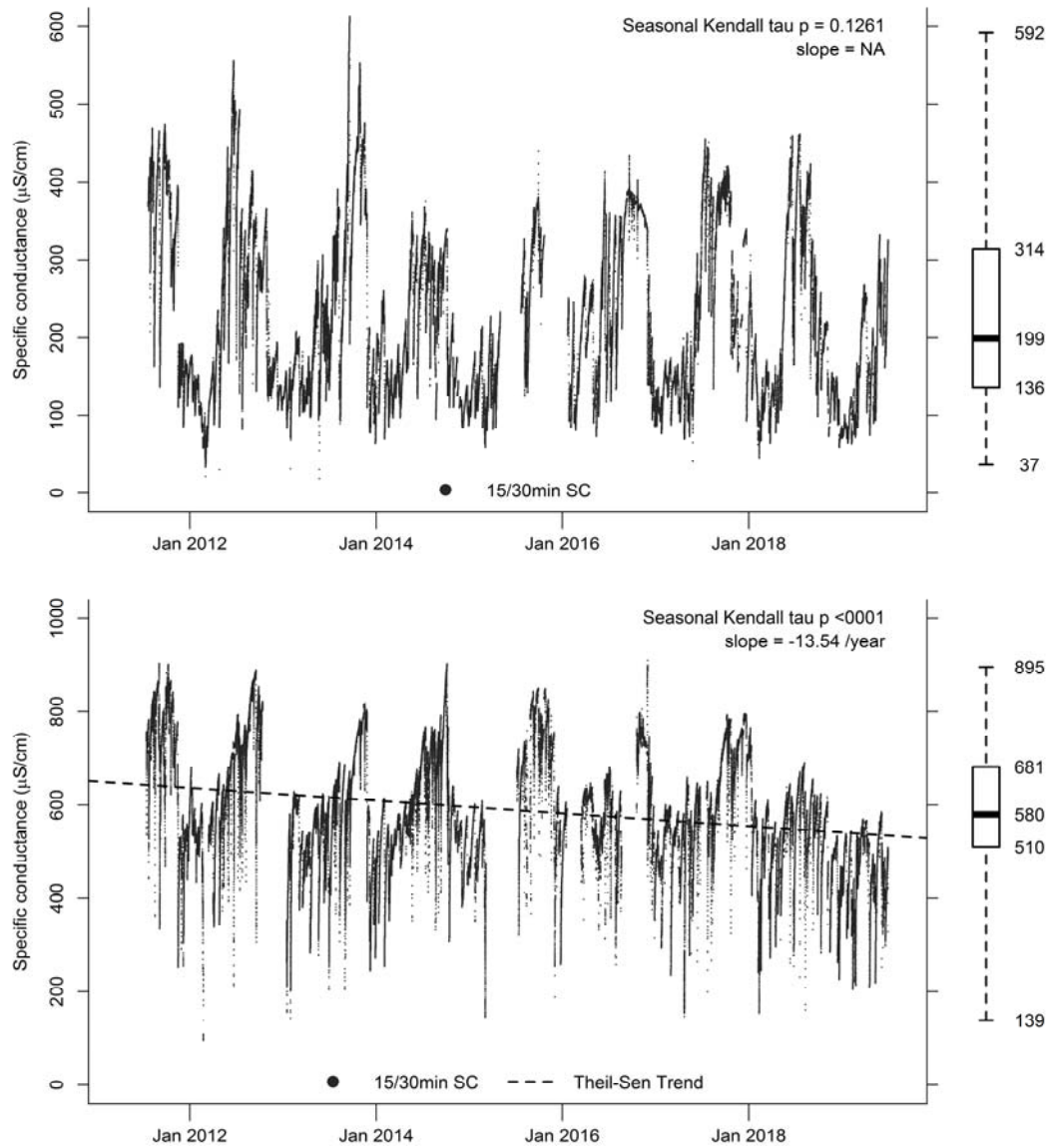


Figure 1: Examples of temporal trends in weekly mean specific conductance (SC) across 23 central Appalachian headwater streams from fall 2011 to summer 2019. No change in SC (top). Decreasing trend in SC (bottom). Seasonal Kendall tau P-value and Theil-Sen trend (dashed line) if statistically significant ($P < 0.05$). Boxplot of 15/30 minute continuous SC showing interquartile range, extreme values, and median.

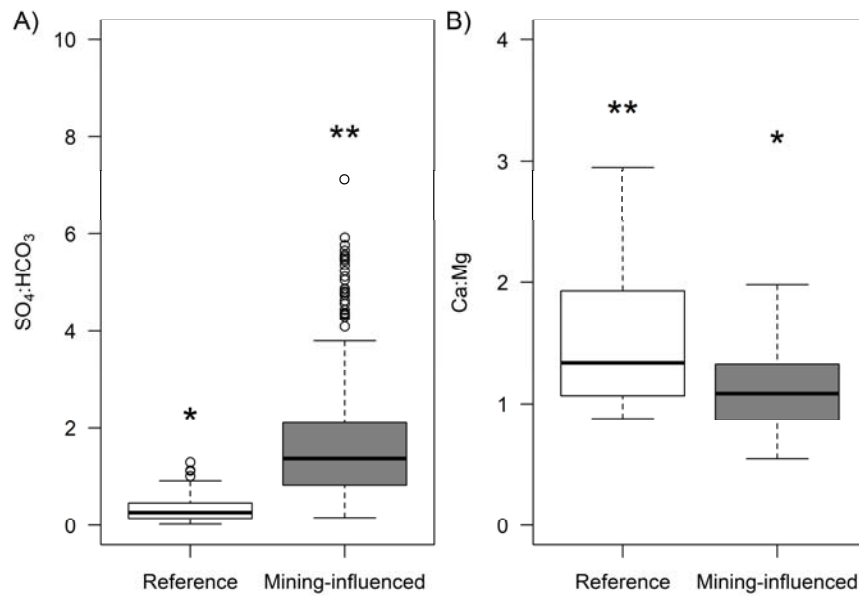


Figure 2: Ion matrix in five reference and 18 mining-influenced streams in the central Appalachian coalfield from fall 2011 to spring 2018. A) mmol ratio of SO₄:HCO₃ and B) mmol ratio of Ca:Mg in reference and mining-influenced streams. For each panel, difference in the number of asterisks denote significant difference based on a linear mixed-effects model with study stream defined as a random variable, alpha = 0.05.

Benthic Macroinvertebrates

We used spearman correlations to test our prediction that the selected biological metrics would decrease with increasing salinity. During spring seasonal sampling across all years, there was a highly significant ($p < 0.01$) negative correlation between SC measured at the time of sampling and the selected biological metrics (Table 4). Correlations were not as strong in the fall for scraper richness or Shannon diversity. In fall of 2012 and 2013, there was no significant relationship between SC and scraper richness. In fall 2013, there was no significant relationship between SC and Shannon diversity. The test stream RFF was excluded from all analyses of benthic macroinvertebrate communities because of removal of the riparian buffer and increased sedimentation observed after Fall 2017.

Temporal trends in biological metrics were analyzed using mixed models, with few observed significant trends. Reference streams only had two significant trends in biological metrics over the study period (one positive trend in richness and one decreasing trend in scraper richness; Table B-1). Test streams had a total of 14 positive trends and five negative trends over the five-year span of study. Shannon diversity had the most trends across sites with four positive trends found at test streams. Scraper richness had no positive trends and one negative trend.

Table 2: Spearman correlations between specific conductance and selected benthic macroinvertebrate metrics across 23 study headwater streams in the central Appalachian coalfield using seasonal fall and spring sampling during five years.

| Metric | Fall | | | | | Spring | | | | |
|--------------------------------------|--------|--------|--------|--------|--------|--------|--------|--------|--------|--------|
| | 2011 | 2012 | 2013 | 2015 | 2017 | 2012 | 2013 | 2014 | 2016 | 2018 |
| Richness | -0.75* | -0.51* | -0.78* | -0.56* | -0.77* | -0.75* | -0.76* | -0.72* | -0.66* | -0.74* |
| EPT** richness | -0.80* | -0.62* | -0.71* | -0.59* | -0.71* | -0.81* | -0.81* | -0.81* | -0.82* | -0.76* |
| Ephemeroptera richness | -0.80* | -0.76* | -0.79* | -0.82* | -0.80* | -0.87* | -0.88* | -0.83* | -0.93* | -0.80* |
| Ephemeroptera richness less Baetidae | -0.84* | -0.73* | -0.75* | -0.81* | -0.80* | -0.86* | -0.88* | -0.88* | -0.88* | -0.77* |
| %Ephemeroptera less Baetidae | -0.85* | -0.74* | -0.76* | -0.83* | -0.83* | -0.84* | -0.89* | -0.90* | -0.89* | -0.78* |
| scraper richness | -0.61* | -0.39 | -0.33 | -0.53* | -0.69* | -0.71* | -0.59* | -0.74* | -0.74* | -0.73* |
| Shannon diversity | -0.61* | -0.41 | -0.55* | -0.55* | -0.60* | -0.61* | -0.67* | -0.76* | -0.71* | -0.67* |
| % Ephemeroptera | -0.73* | -0.79* | -0.76* | -0.84* | -0.78* | -0.69* | -0.87* | -0.86* | -0.83* | -0.84* |

*P-value <0.05, **EPT- calculated as the total number of distinct taxa from three orders of macroinvertebrates: 1) Ephemeroptera (mayflies), 2) Plecoptera (stoneflies), and 3) Trichoptera (caddisflies).

We assessed association between improving water quality and recovery of macroinvertebrate communities by overlapping temporal trends in SC and biological metrics in the 18 mining-influenced streams. The five streams with decreasing SC (i.e., improving water quality) corresponded with few positive trends in biological metric scores (i.e., recovery of macroinvertebrate communities) (Figure 3). For community-level metrics (richness, scraper richness, EPT richness, and Shannon diversity), there were two positive trends and one negative trend observed in streams with decreasing SC (Figure 3A). Mining-influenced streams with no change in SC showed some change in community-level metrics, with six positive trends and no negative trends.

The four metrics that exclusively measure Ephemeroptera taxa (%Ephemeroptera less Baetidae, %Ephemeroptera, Ephemeroptera richness, and Ephemeroptera richness less Baetidae) showed less response to decreasing trends in SC compared to the community-level metrics (Figure 3B). For these four Ephemeroptera-specific metrics, all five mining-influenced streams with decreasing SC had no significant trends in metric scores. However, the other 13 mining-influenced streams with no temporal trends in SC showed some changes in Ephemeroptera metrics with six positive and three negative trends.

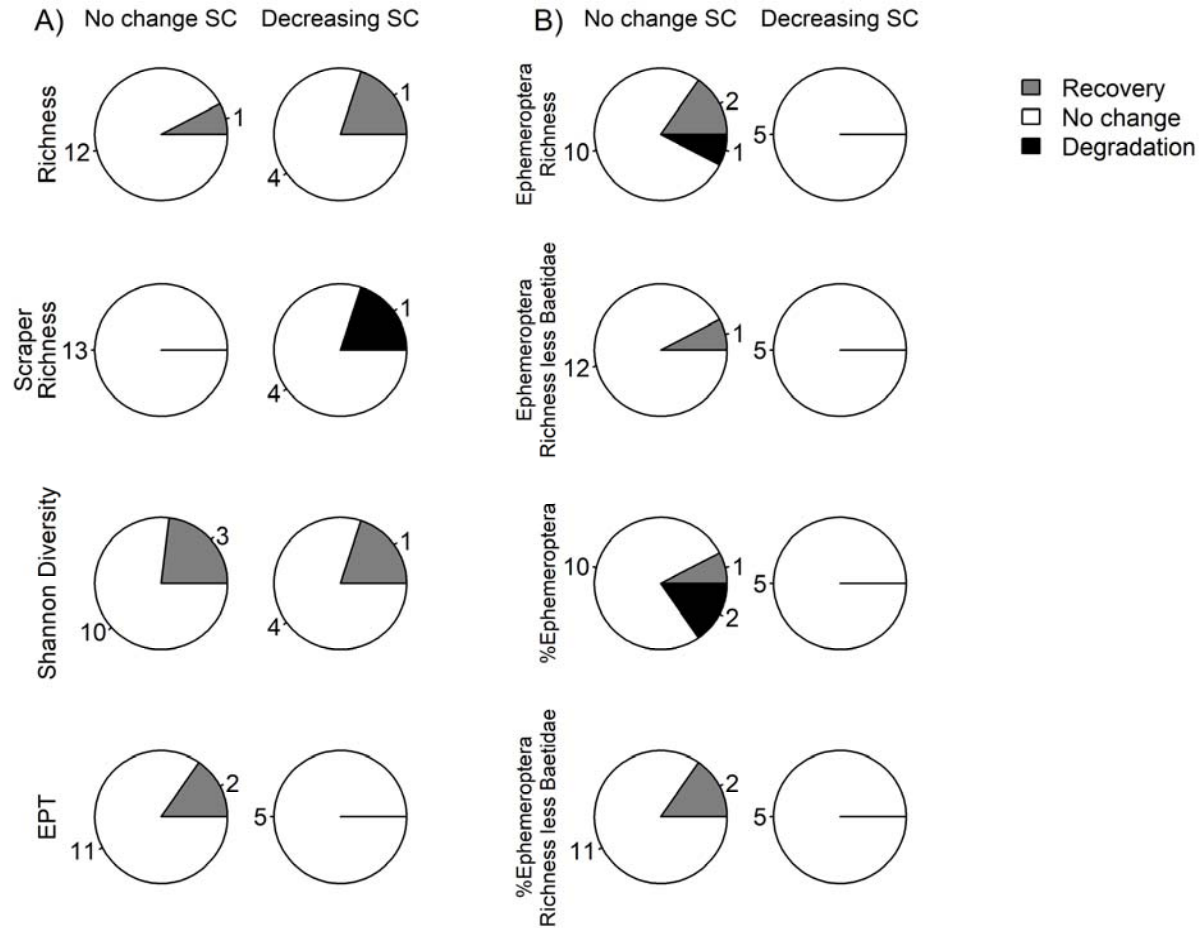


Figure 3: Temporal trends in A) benthic macroinvertebrate community-level metrics and B) Ephemeroptera-specific metrics for mining-influenced streams with no change in SC (n=13) and those with decreasing SC trends (n=5) from fall 2011 to summer 2019. White denotes proportion of these stream categories with no change in listed biological metrics, gray denotes proportion with positive trends (i.e., recovery), and black denotes proportion with negative trends (i.e., degradation).

Spatial Patterns in Water Chemistry

HUR

Stream network length was the same in HUR between baseflow and highflow sampling events (Figure 5a,b). At the bottom of the sampled stream network, SC was 335 $\mu\text{s}/\text{cm}$ under baseflow compared to 232 $\mu\text{s}/\text{cm}$ under highflow, suggestive of flow differences during these periods. Under baseflow, SC was influenced by tributary inputs. Tributaries 3 and 4 added water dilute in SC, resulting in lower SC values in the mainstem after confluences with these tributaries. However, tributary 5, which is proximate to the valley fill in this watershed, had the highest SC (732 $\mu\text{s}/\text{cm}$) and contributed to a 49% increase in SC in the mainstem under baseflow conditions (Figure 5c). Because of increased SC from this tributary, SC was 16% greater at the most downstream sampled location (at the *in-situ* datalogger) than the stream origin. However, major

ions did not always follow the spatial pattern observed for SC. For example, tributary 3, although more dilute in SC than the mainstem, had increased concentrations of Mg, Cl, and SO₄ (Figure C-1). The high-SC tributary 5 enriched Mg, SO₄, and Ca in the mainstem while further diluting Na. Tributaries had less of an effect on the concentrations of trace elements. All trace elements except for Mn, Fe, and Ba showed patterns of dilution with distance downstream from stream origin (Figure C-2).

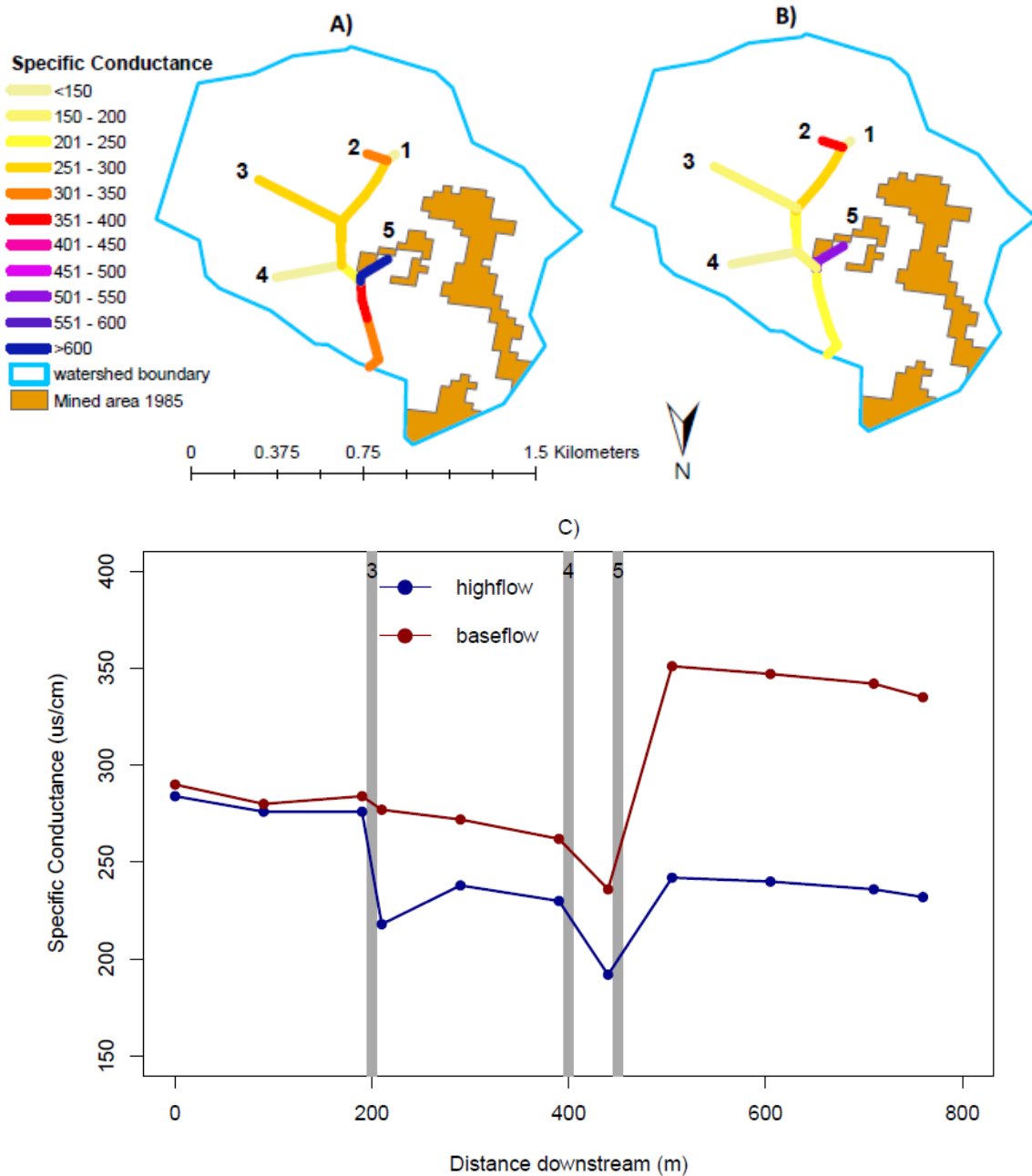


Figure 5: Spatial maps of specific conductance (SC) under (A) baseflow and (B) highflow conditions for Hurricane Branch, VA. (C) Specific conductance with distance downstream under baseflow and highflow. Tributaries are marked with gray-shaded lines and labeled with numbers corresponding to location in figures (A) and (B).

During highflow conditions, there was more dilution in SC with distance downstream compared to baseflow conditions (Figure 5c). However, in the furthest upstream part of the stream network, tributary 2 had slightly higher SC under highflow indicating source activation ($384 \mu\text{s}/\text{cm}$ at highflow vs. $331 \mu\text{s}/\text{cm}$ at baseflow) (Figure 5b). Note that tributary 2 is not shown in Figure 5c, which begins below the confluence of tributaries 1 and 2. Consequently, at upstream sample locations, SC was nearly identical to baseflow conditions before substantial dilution from tributaries 3 and 4 (Figure 5c). Tributary 5 still contributed water with elevated SC but its effect on mainstem SC was less than at baseflow, contributing to a 26% increase in SC. Unlike baseflow, SC was 18% less at the downstream sample location compared to the stream origin. All major ions, except for Mg and Cl, generally decreased in concentrations with distance downstream under highflow (Figure C-1). Spatial patterns of individual major ion enrichment and dilution in tributaries were similar under baseflow and highflow. Similarly, trace elements generally showed similar patterns of downstream dilution as observed during baseflow conditions (Figure C-2).

Comparing concentrations between flow conditions demonstrated that highflow generally resulted in lower major ion concentrations compared to baseflow (Figure C-1). Chloride was the one exception to this trend with increased concentrations under highflow at every sample location. The relative dilution of most major ions under highflow increased with distance downstream. In contrast, relative concentrations of trace elements were more variable (Figure C-2). Strontium and Ba had spatial patterns similar to major ions with concentrations becoming increasingly dilute with highflow, whereas other elements (i.e., B, Mn, Fe, and Zn) were consistently enriched compared to baseflow conditions. Manganese showed the most enrichment being approximately two times higher in concentration at the downstream sampling location under highflow compared to baseflow conditions.

LLE

Stream network length was the same in LLE across baseflow and highflow sampling events (Figure 6a,b). Specific conductance measured at the bottom of the sampled stream network was $280 \mu\text{s}/\text{cm}$ under baseflow and $209 \mu\text{s}/\text{cm}$ under highflow. Similar to SC patterns in HUR, SC was influenced by tributary inputs in LLE under baseflow conditions (Figure 6c). Tributary 2 reduced SC by half in the mainstem, whereas tributaries 3 and 4 both increased SC in the mainstem. Tributary 4, although the shortest tributary, had the highest SC of any part of the stream network and increased SC in the mainstem by 42% under baseflow conditions. In the absence of tributaries, SC generally decreased with distance downstream. The overall decrease in SC under baseflow conditions did not necessarily correspond to dilution in major ion concentrations. For example, Na was enriched throughout the stream network as a result of increased contributions from all tributaries (Figure C-3). Bicarbonate was also enriched at the bottom of the stream network compared to the origin as a result of high inputs from tributary 4. Trace elements were more variable in concentration across the stream network compared to major ions (Figure C-4). Tributary 3 contributed elevated Al and Mn concentrations to the mainstem, which remained enriched at the bottom of the sampled stream network. Tributary 4 had a similar effect on Sr concentrations.

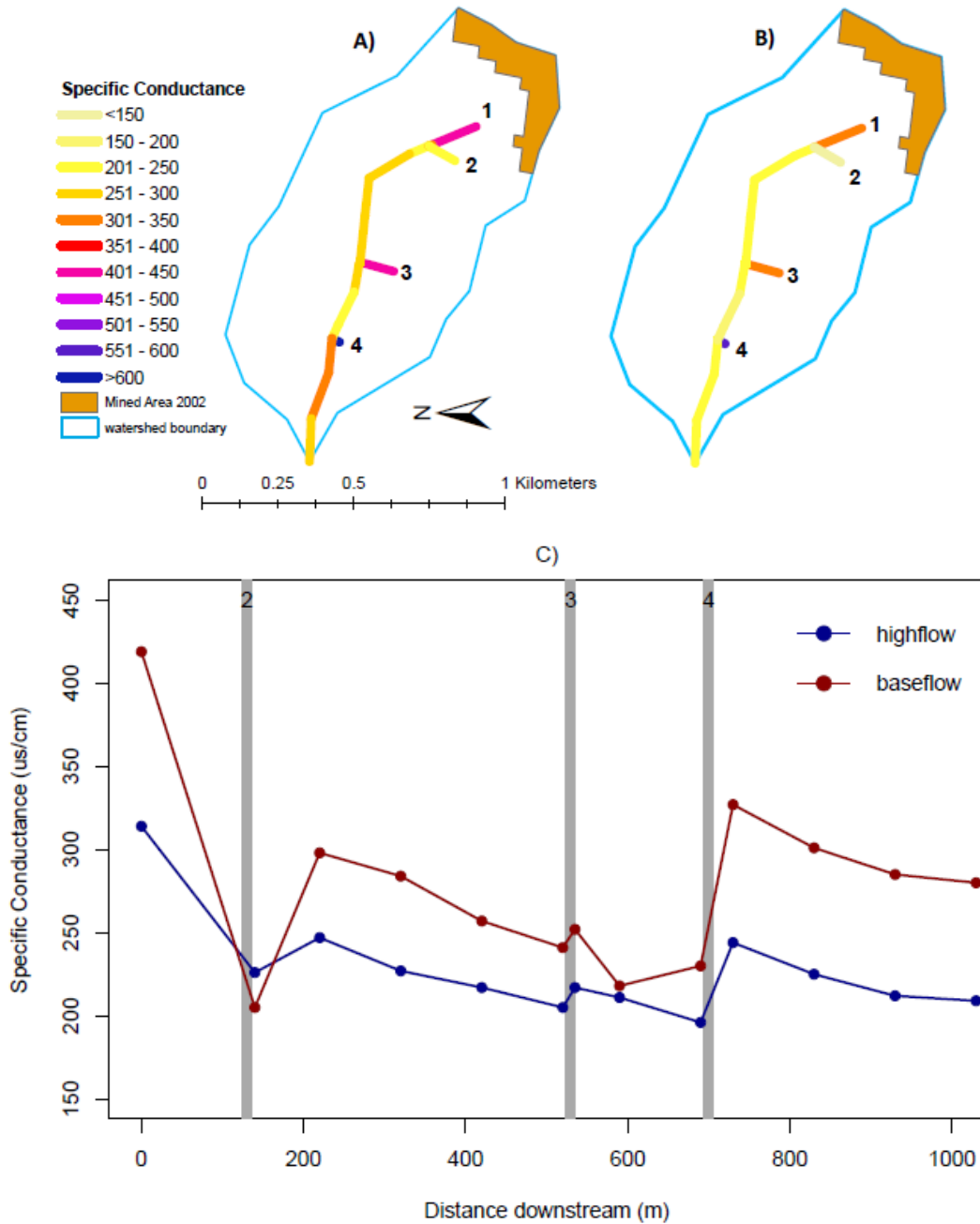


Figure 6: Spatial maps of specific conductance (SC) under (A) baseflow and (B) highflow conditions for Longlick Branch East Fork, WV. (C) Specific conductance with distance downstream under baseflow and highflow. Tributaries are marked with gray-shaded lines and labeled with numbers corresponding to location in figures (A) and (B).

During highflow conditions, there was also a general dilution in SC with distance downstream (Figure 6b,c). However, the effects of tributaries were reduced compared to baseflow conditions. For example, tributary 1, which reduced SC by half under baseflow, resulted in only a 28% reduction under highflow. Similarly, tributary 5 contributed to a 24% increase in SC during highflow compared to 42% under baseflow. Sodium was the only major ion to be enriched at the most downstream sampled location compared to origin concentrations (Figure C-3). The other major ions followed the trend of SC dilution along the stream network. Highflow had a greater impact on relative concentrations of trace elements than the major ions (Figure C-4). Aluminum, while enriched under baseflow, was diluted under highflow. Manganese, B, and Sr were all enriched at the bottom of the stream network during highflow.

When directly comparing baseflow and highflow conditions, concentrations of all major ions excluding Na, were increased under highflow near the stream origin after the confluence of tributary 2 (Figure C-3). However, below this sample location, most major ion concentrations became more dilute. Conversely, K remained enriched relative to baseflow concentrations at every sample location. Trace element concentrations were more variable than major ions (Figure C-4). Strontium and Ba had patterns similar to the majority of major ions, with lower concentrations under highflow compared to baseflow conditions. Conversely, concentrations of B and Mn were higher during highflow than at baseflow at every sample location.

ROL

In contrast to the other two stream networks sampled, ROL had an expanded network length under highflow, including three tributaries that were dry under baseflow (Figure 7a,b). Specific conductance measured at the bottom of the watershed was 462 $\mu\text{s}/\text{cm}$ under highflow and 662 $\mu\text{s}/\text{cm}$ under baseflow. Tributary 1 was the only tributary present under baseflow (Figure 7a). For baseflow conditions, this tributary had lower SC than the mainstem (1,003 vs. 1,230 $\mu\text{s}/\text{cm}$) yet only contributed a 6% reduction in SC (Figure 7c). Specific conductance declined by 62% from stream origin to the most downstream location during baseflow conditions. Of the major ions sampled in this stream network, Ca, K, and Mg followed the same dilution pattern as SC (Figure C-5). Conversely, Na was enriched throughout the stream network downstream of tributary 1. Trace element concentrations were more variable than major ions (Figure C-6). Selenium showed dilution relative to initial concentrations, Ba was enriched throughout the stream network, and Mn, Fe, and Al were variable with spikes of enrichment in several sample locations.

Under highflow, the stream network length increased, and three tributaries that were dry under baseflow were sampled (Figure 7b). Tributaries 2, 3, and 4 had lower SC than the mainstem whereas tributary 1, which had lower SC than the mainstem under baseflow, had higher SC than the mainstem under highflow. Despite lower SC at each sample location, we observed a similar pattern of SC reduction by 58% from stream origin to the downstream sampling location under highflow. After initial enrichment of Mg and Na near the stream origin, we observed dilution of all major ions sampled compared to origin concentrations (Figure C-5). Trace elements concentrations under highflow displayed similar patterns to baseflow, except for Ba, which was diluted relative to origin concentration (Figure C-6).

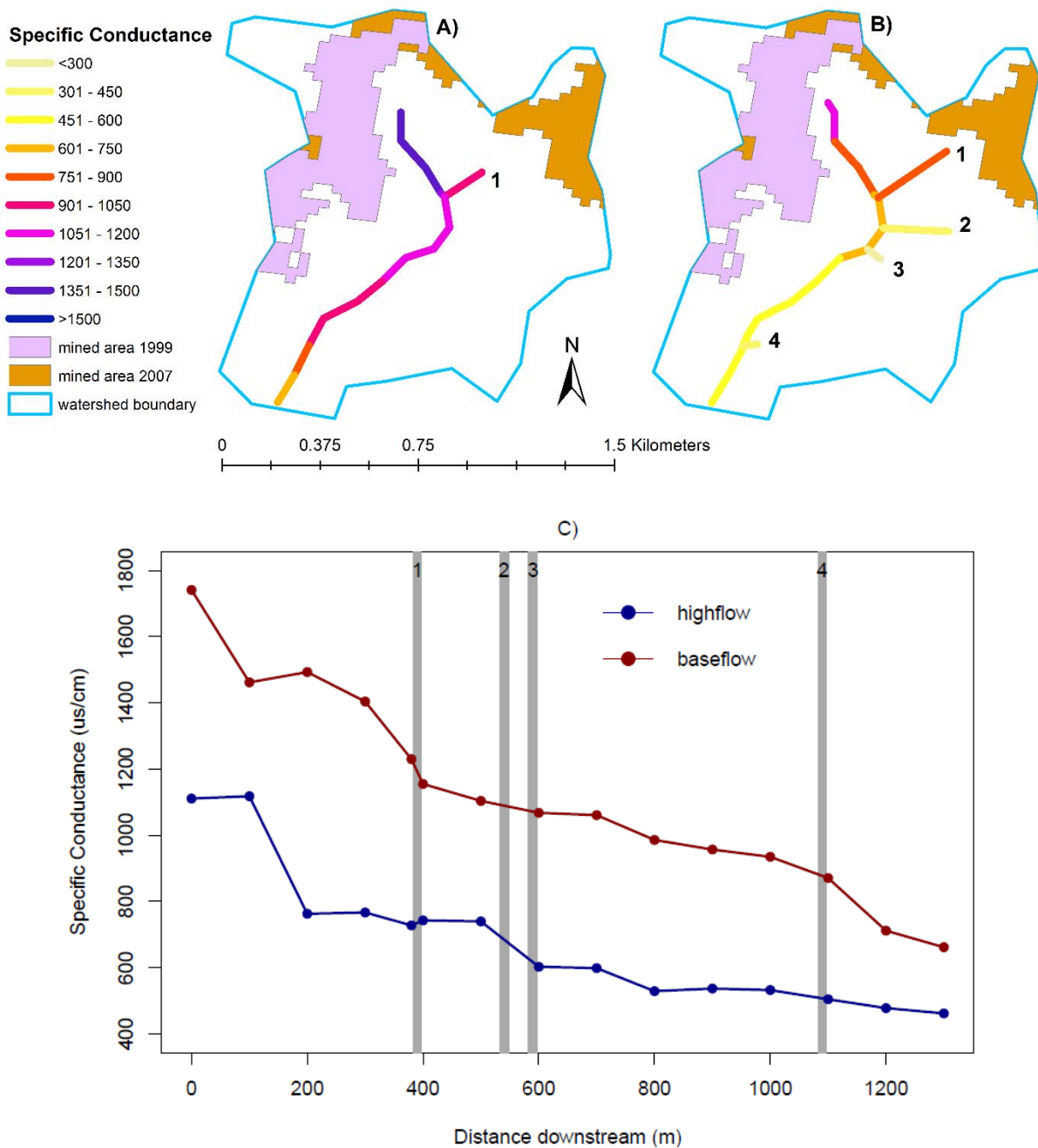


Figure 7: Spatial maps of specific conductance (SC) under (A) baseflow and (B) highflow at Roll Pone Branch, VA. (C) Specific conductance with distance downstream under baseflow and highflow. Tributaries are marked with gray-shaded lines and labeled with numbers corresponding to location in figures (A) and (B).

A direct comparison between baseflow and highflow conditions demonstrated lower major ion concentrations at the bottom of the stream network during highflow; however, K had the least dilution under highflow compared to the other major ions (Figure C-5). Sodium, K, and Mg had

initial enrichment near the stream origin with highflow, but concentrations became lower compared to baseflow concentrations moving downstream. Trace element concentrations were more variable than major ion concentrations (Figure C-6). All trace element concentrations at the stream origin, except for Mn, were elevated under high flows compared to baseflow. Differences between baseflow and highflow Se were variable throughout the stream network. Iron, Mn, Al, and Zn were enriched with highflow at the bottom of the watershed with Mn concentration being approximately nine times higher than baseflow concentrations at the furthest downstream sample location.

DISCUSSION

In this work, we assessed temporal trends in water chemistry and benthic macroinvertebrate communities across 23 headwater streams during a seven-year period in the central Appalachian coalfield. In addition, we evaluated spatial and flow-driven variation in water chemistry at a subset of three surface mining-influenced headwater streams. Results indicate that surface coal mining has long-term impacts on water chemistry and benthic macroinvertebrate communities in central Appalachian headwater streams. Some test streams in this study had gradual decreasing trends in SC measured between fall 2011 and summer 2019. However, benthic macroinvertebrates, particularly Ephemeroptera and scrapers, showed little response to these improvements. A limitation of this study is that measurements of water chemistry and benthic macroinvertebrate communities were made at one location within each stream. To that end, our results further demonstrate that water chemistry is variable within a stream reach and under different flow conditions, highlighting future research needs to better characterize impacts of surface mining across entire stream networks.

Temporal Trends in SC, Ion Matrix, and Benthic Macroinvertebrates

We evaluated long-term SC trends (fall 2011 to summer 2019) in both mining-influenced and reference streams to assess recovery following surface mining considering natural water chemistry variation. Undisturbed, central Appalachian headwater streams naturally vary in salinity over time in response to such factors as climatic conditions and thus flow variation (Timpano et al. 2018a). Indeed, Timpano et al. (2018a) found salinity deviations of $\pm 20\%$ of annual mean SC with maximum and minimum SC occurring in late summer and late winter, respectively. Despite interannual variation in SC, we found only one significant long-term SC trend in our reference streams, albeit with small magnitude of imputed annual change, indicating relatively stable seasonal levels of SC among years.

Temporal trend analysis of our 18 mining-influenced streams suggests little recovery of water quality conditions over the 8-year study period. Five mining-influenced streams had decreasing long-term trends in SC, and at annual rates exceeding reference conditions, thus indicating possible recovery from mining conditions. However, the magnitude of SC decline in these streams suggests long recovery times (ca. decades) to return to “reference conditions”. The average annual mean SC of the five streams with decreasing SC was $707 \mu\text{s}/\text{cm}$ with an average trend of $-16 \mu\text{s}/\text{cm yr}^{-1}$. Assuming that these temporal trends remain constant over time, it would

take approximately 25 years for these streams to have annual mean SC < 300 $\mu\text{s}/\text{cm}$, which has been established as the regional stream SC benchmark (USEPA 2011b). Moreover, it would take ca. 40 years for these streams to reach the average annual mean SC of the reference streams in this study (67 $\mu\text{s}/\text{cm}$). At the mining-influenced stream KUT (annual mean SC = 1,068 $\mu\text{s}/\text{cm}$), there was a decreasing trend of -20 $\mu\text{s}/\text{cm yr}^{-1}$, suggesting ca. 40 years for this stream to reach an annual mean SC lower than the EPA benchmark and 50 years to reach observed reference conditions. Further, 13 mining-influenced streams had no change over the eight-year study, indicating long-term impacts from surface mining and highlighting the need for continued monitoring of these streams over longer time periods.

Along with declines in SC, changes in ion matrix can occur in streams following termination of mining activity and with continued weathering of waste material. For example, we expected that $\text{SO}_4:\text{HCO}_3$ ratios would decline over time based on previous laboratory studies showing that sulfate is the dominant anion early in the leaching process of mine spoils and slowly decreases in concentration with repeated leaching events (Orndorff et al. 2015; Daniels et al. 2016). Thus, observed negative trends in $\text{SO}_4:\text{HCO}_3$ ratios at some of the mining-influenced streams suggests weathering of overburden rock and thus possible recovery. However, six mining-influenced streams showed no significant trends, concordant with their lack of SC trends. We also expected that the Ca:Mg ratio would increase over time as a result of aging mine spoils and a gradual return to reference-like conditions. However, we found no increasing trends for Ca:Mg in mining-influenced streams.

Despite some mining-influenced sites showing slow recovery of water quality conditions, we found limited evidence of coincident recovery of benthic macroinvertebrate communities over the study period. Benthic macroinvertebrate community metrics, particularly metrics for Ephemeroptera groups, were negatively affected by SC across mining-influenced streams during fall and spring seasonal sampling periods. However, these biological metrics showed little response in the streams with decreasing SC trends. Four Ephemeroptera metrics had no significant positive trends present in streams with decreasing SC and had few trends present in streams with no change in SC. The four biological metrics that do not focus on Ephemeroptera taxa, also showed limited response to decreasing SC. For these metrics, only one of five streams with decreasing SC had associated positive trends in metric scores. Further, scraper richness showed no positive trends in sites with decreasing SC.

Absence of positive trends (i.e., biological recovery) in Ephemeroptera metrics in mining-influenced streams is important to note because of the well-documented decline of sensitive Ephemeroptera taxa in headwater streams influenced by surface mining in central Appalachia (Merricks et al. 2007; Pond et al. 2008, 2010, 2014; Timpano et al. 2015, 2018b). Similarly, the scraper functional feeding group has been shown to be reduced in mining-influenced streams, primarily as a result of the loss of several Ephemeroptera scraper taxa (Pond et al. 2014; Timpano et al. 2018b). These results suggest that sensitive benthic macroinvertebrates (i.e., scrapers and Ephemeroptera) may have limited recovery despite gradual recovery of water chemistry (i.e., decreases in SC and $\text{SO}_4:\text{HCO}_3$). However, we critically note the difference between measures of temporal trends in 30-minute, continuous SC data compared to estimated

trends in biological metrics using only seasonal sampling. A sampling approach with higher resolution (e.g., monthly) of macroinvertebrate community metrics may be more effective at identifying temporal trends in biological metrics (Boehme et al. 2016).

Specific conductance may not be the only stressor to benthic macroinvertebrates in these headwater streams. Drover (2018) found significant, negative correlations of Ephemeroptera and scraper richness metrics with water-column selenium (Se) concentrations in a subset of the same central Appalachian headwater streams used in this study. Selenium is a naturally occurring trace element but can be elevated to potentially harmful levels in streams influenced by surface mining (USEPA 2016) and has been shown to bioaccumulate to potentially toxic levels in benthic macroinvertebrates (DeBruyn and Chapman 2007; Conley et al. 2009; Whitmore et al. 2018; Cianciolo et al. 2019 in review). In particular, Se can bioaccumulate into stream biofilm (Arnold et al. 2017; Whitmore et al. 2018), which is consumed by scrapers and several sensitive Ephemeroptera taxa. Therefore, it is possible that Se is an additional stressor to these groups, potentially explaining some of the discrepancy between gradual recovery in water chemistry (i.e., decreasing SC) and absence of positive trends in biological metrics, particularly in Ephemeroptera and scrapers.

Spatial Patterns in Water Chemistry

Water chemistry in surface mining-influenced headwater streams varies spatially within stream networks. In the absence of tributaries, we observed a general dilution pattern in SC and dissolved major ion concentrations with distance downstream from mined areas under both highflow and baseflow conditions. We suspect this is a result of more dilute groundwater from less intensively mined areas, which increasingly contributes to flow with distance downstream from surface mining activities. For example, in the ROL site, SC after the confluence with Tributary 1 was reduced by 43% under baseflow conditions likely caused by groundwater dilution. Similar patterns, albeit less pronounced, were observed in the other two study streams evaluated for spatial patterns. In addition to groundwater input, tributaries also influenced dissolved ion concentrations, resulting in both enrichment and dilution in our study streams. At site LLE, three tributaries contributed SC-enriched streamwater under highflow and baseflow. Tributary 4 at this site had SC approximately three times higher than the mainstem under baseflow. Conversely, ROL had three dilute tributaries at highflow contributing to lower SC in the mainstem. At site HUR, tributary 5 originating below a valley fill increased the mainstem SC by 49% under baseflow. These results show that tributaries and groundwater can have substantial influence on the salinity of headwater streams by adding water enriched or diluted in dissolved ions.

Flow conditions can also contribute to water chemistry variation within surface mining-influenced stream networks. In the mainstems of the three sampled stream networks, major ion concentrations and SC were typically lower under highflow compared to baseflow conditions and were conservative, tracking with salinity (i.e., SC) at each sample location. Similarly, the majority of tributaries sampled in this study had lower SC and dissolved ion concentrations under highflow conditions. However, one tributary became more enriched with highflow, which

likely extended groundwater and surface water networks into new sources of high concentrations of dissolved ions (e.g., recent valley fill material) (Paybins 2003).

Our results highlight key drivers of downstream water chemistry in surface mining-influenced watersheds by demonstrating: i) general conservative behavior of major ions, ii) locations and times for elevated ion contribution from specific tributaries, and iii) groundwater dilution from relatively undisturbed areas. Potential downstream consequences for larger, mixed-land use watersheds have been explored by other studies in the central Appalachian coalfield. For example, Johnson et al. (2019) sampled 60 sites in one large eastern Kentucky watershed influenced by surface mining. The authors found high variability in major ions in small sub-watersheds <math><15 \text{ km}^2</math>, but then convergent patterns across larger sub-watersheds (>75 km²) as streams merged into larger orders. Their research and complimentary modeling work (Johnson et al. 2010) suggest that downstream water chemistry represents a mix of land-use activities in headwater catchments and that undisturbed streams provide a vital source of water diluted in dissolved ions. However, this previous work does not directly address the local-scale influence of tributaries and groundwater on dissolved ion concentrations or SC within a watershed or even within a stream reach. Our data indicate that these sources for enrichment or dilution can have an influence on dissolved ion concentrations within small headwater watersheds and point to future work to better understand emergent outcomes for downstream water quality.

Despite observations of increased major ion loading from surface mining in the central Appalachian coalfield (Johnson et al. 2010, 2019), less is known about delivery and downstream variation of trace elements, which can have important implications for the condition of aquatic communities. Spatial patterns of trace elements were different than patterns of major ions throughout our three sampled streams and largely did not track with patterns in SC. Strontium was a notable exception showing conservative patterns in each stream more akin to major ions than the other trace elements. Several trace elements (i.e., Al, Zn, Al, and Fe) had variable concentrations throughout the stream network under both highflow and baseflow conditions. In contrast, downstream Mn concentrations were consistently enriched above stream-origin concentrations in all streams. Concentrations of Mn were also higher under highflow compared to baseflow at the bottom of the stream network in all streams. The lack of dilution of many trace elements and enrichment of others under highflow could have negative, downstream impacts for biological communities. For example, native mussels show decline in richness and abundance in the Clinch and Powell Rivers (Ahlstedt et al. 2005), which have headwaters originating in the central Appalachian coalfield. Elevated concentrations of major ions are likely not the major driver of mussel decline in these rivers (Ciparis et al. 2015). Instead, it has been suggested that chronically elevated concentrations of certain trace elements are a potential cause for regional native mussel decline (Naimo 1995; Zipper et al. 2016). Our findings suggest that future work is needed to address delivery of potentially toxic trace elements from surface mining-influenced headwaters to downstream waters.

CONCLUSION

Results from 23 headwater streams in the central Appalachian coalfield suggest that surface coal mining impacts water chemistry and benthic macroinvertebrate communities for at least decades

after mining activities cease. We found limited evidence of declining temporal trends in salinity across 18 mining-influenced headwater streams over an 8-year period. The magnitude of negative trends in salinity that were observed suggest recovery times on the order of decades for conditions to return to those observed in reference streams. Moreover, the study streams with negative trends in salinity often did not have associated recovery of benthic macroinvertebrate communities. Ephemeroptera and scrapers appear to be the most sensitive of the measured benthic macroinvertebrate metrics to elevated salinity over time. Continuation of this long-term dataset, which is unique in its scope and length, would be invaluable for expanding our understanding of the long-term impacts of surface mining on headwater streams.

The high-resolution spatial sampling of SC, major ions, and trace elements in a subset of three surface mining-influenced headwater streams demonstrated that water chemistry varies substantially within these small watersheds (< 1.5 km²). Our results suggest that it is imperative to consider when (i.e., flow conditions) and where (i.e., location in the watershed) water and benthic macroinvertebrate samples are collected to assess stream condition. The marked spatial variability in water chemistry that we observed within surface mining-influenced streams suggests future work to address associated variability in benthic macroinvertebrate community structure. Trace elements did not show the same conservative, dilution patterns of major ions and can be enriched with potential implications for the condition of aquatic organisms in higher-order systems downstream of surface mining. Continuing research into the interaction between groundwater, surface water, and weathering overburden waste rock is needed to expand knowledge of spatial and flow-variation in water chemistry and aquatic biota in surface mining-influenced headwater streams.

LITERATURE CITED

- Ahlstedt, S. A., Fagg, M. T., Butler, R. S., & Connell, J. F. (2005). Long-term trend information for freshwater mussel populations at twelve fixed-station monitoring sites in the Clinch and Powell rivers of Eastern Tennessee and Southwestern Virginia 1979–2004. *Final Report, US Fish and Wildlife Service, Cookeville, TN, 38501*.
- American Public Health Association (APHA). 2005. Standard methods for the examination of water and wastewater. 21st ed. American Public Health Assoc., Washington, DC.
- Arnold, M. C., Bier, R. L., Lindberg, T. T., Bernhardt, E. S., & Di Giulio, R. T. (2017). Biofilm mediated uptake of selenium in streams with mountaintop coal mine drainage. *Limnologica*, 65, 10-13.
- Barbour, M. T., Gerritsen, J., Snyder, B. D., & Stribling, J. B. (1999). *Rapid bioassessment protocols for use in streams and wadeable rivers: periphyton, benthic macroinvertebrates and fish* (2nd ed., p. 339). Washington, DC: US Environmental Protection Agency, Office of Water.
- Beggel, S., & Geist, J. (2015). Acute effects of salinity exposure on glochidia viability and host infection of the freshwater mussel *Anodonta anatina* (Linnaeus, 1758). *Science of the Total Environment*, 502, 659-665.
- Blakeslee, C. J., Galbraith, H. S., Robertson, L. S., & St John White, B. (2013). The effects of salinity exposure on multiple life stages of a common freshwater mussel, *Elliptio complanata*. *Environmental Toxicology and Chemistry*, 32(12), 2849-2854.
- Boehme, E. A., Zipper, C. E., Schoenholtz, S. H., Soucek, D. J., & Timpano, A. J. (2016). Temporal dynamics of benthic macroinvertebrate communities and their response to elevated specific conductance in Appalachian coalfield headwater streams. *Ecological Indicators*, 64, 171-180.
- Burton, J., & Gerritsen, J. (2003). A stream condition index for Virginia non-coastal streams. *Virginia Department of Environmental Quality, Richmond, Virginia, USA*.
- Cañedo-Argüelles, M., Hawkins, C. P., Kefford, B. J., Schäfer, R. B., Dyack, B. J., Brucet, S., ... & Coring, E. (2016). Saving freshwater from salts. *Science*, 351(6276), 914-916.
- Ciparis, S., Phipps, A., Soucek, D. J., Zipper, C. E., & Jones, J. W. (2015). Effects of environmentally relevant mixtures of major ions on a freshwater mussel. *Environmental Pollution*, 207, 280-287.
- Clark, E. V., Daniels, W. L., Zipper, C. E., & Eriksson, K. (2018a). Mineralogical influences on water quality from weathering of surface coal mine spoils. *Applied Geochemistry*, 91, 97-106.
- Clark, E. V., Zipper, C. E., Daniels, W. L., & Keefe, M. J. (2018b). Appalachian coal mine spoil elemental release patterns and depletion. *Applied Geochemistry*, 98, 109-120.

- Conley, J. M., Funk, D. H., & Buchwalter, D. B. (2009). Selenium bioaccumulation and maternal transfer in the mayfly *Centroptilum triangulifer* in a life-cycle, periphyton-biofilm trophic assay. *Environmental Science & Technology*, 43(20), 7952-7957.
- Daniels, W. L., Zipper, C. E., Orndorff, Z. W., Skousen, J., Barton, C. D., McDonald, L. M., & Beck, M. A. (2016). Predicting total dissolved solids release from central Appalachian coal mine spoils. *Environmental Pollution*, 216, 371-379
- DeBruyn, A. M., & Chapman, P. M. (2007). Selenium toxicity to invertebrates: will proposed thresholds for toxicity to fish and birds also protect their prey?. *Environmental Science & Technology*, 41(5), 1766-1770.
- Driscoll, C. T., Driscoll, K. M., Roy, K. M., & Mitchell, M. J. (2003). Chemical response of lakes in the Adirondack region of New York to declines in acidic deposition. *Environmental Science & Technology*, 37(10), 2036-2042.
- Drover, D. R. (2018). Benthic macroinvertebrate community structure responses to multiple stressors in mining-influenced streams of central Appalachia USA. (Doctoral dissertation, Virginia Tech).
- Duan, W., He, B., Chen, Y., Zou, S., Wang, Y., Nover, D., Chen, W. and Yang, G., 2018. Identification of long-term trends and seasonality in high-frequency water quality data from the Yangtze River basin, China. *PloS one*, 13(2), p.e0188889.
- Evans, D. M., Zipper, C. E., Donovan, P. F., & Daniels, W. L. (2014). Long-term trends of specific conductance in waters discharged by coal-mine valley fills in central Appalachia, USA. *Journal of the American Water Resources Association*, 50(6), 1449-1460.
- Gerritsen, J., Burton, J., & Barbour, M. T. (2000). A stream condition index for West Virginia wadeable streams. *US EPA Region*, 3.
- Griffith, M. B., Norton, S. B., Alexander, L. C., Pollard, A. I., & LeDuc, S. D. (2012). The effects of mountaintop mines and valley fills on the physicochemical quality of stream ecosystems in the central Appalachians: a review. *Science of the Total Environment*, 417, 1-12.
- Helsel, D. R., & Hirsch, R. M. (2002). *Statistical methods in water resources* (Vol. 323). Reston, VA: US Geological Survey.
- Higgins, C. L., & Wilde, G. R. (2005). The role of salinity in structuring fish assemblages in a prairie stream system. *Hydrobiologia*, 549(1), 197-203.
- Hirsch, R. M., Slack, J. R., & Smith, R. A. (1982). Techniques of trend analysis for monthly water quality data. *Water resources research*, 18(1), 107-121.
- Hirsch, R. M., & Slack, J. R. (1984). A nonparametric trend test for seasonal data with serial dependence. *Water Resources Research*, 20(6), 727-732.

- Johnson, B. R., Haas, A., & Fritz, K. M. (2010). Use of spatially explicit physicochemical data to measure downstream impacts of headwater stream disturbance. *Water Resources Research*, 46(9).
- Johnson, B., Smith, E., Ackerman, J. W., Dye, S., Polinsky, R., Somerville, E., ... & D'Amico, E. (2019). Spatial Convergence in Major Dissolved Ion Concentrations and Implications of Headwater Mining for Downstream Water Quality. *Journal of the American Water Resources Association*.
- Li, J., Zipper, C. E., Donovan, P. F., Wynne, R. H., & Oliphant, A. J. (2015). Reconstructing disturbance history for an intensively mined region by time-series analysis of Landsat imagery. *Environmental Monitoring and Assessment*, 187(9), 557.
- Mann, H. B. (1945). Nonparametric tests against trend. *Econometrica: Journal of the Econometric Society*, 245-259.
- Merricks, T. C., Cherry, D. S., Zipper, C. E., Currie, R. J., & Valenti, T. W. (2007). Coal-mine hollow fill and settling pond influences on headwater streams in southern West Virginia, USA. *Environmental Monitoring and Assessment*, 129(1-3), 359-378.
- Naimo, T. J. (1995). A review of the effects of heavy metals on freshwater mussels. *Ecotoxicology*, 4(6), 341-362.
- Orndorff, Z. W., Daniels, W. L., Zipper, C. E., Eick, M., & Beck, M. (2015). A column evaluation of Appalachian coal mine spoils' temporal leaching behavior. *Environmental Pollution*, 204, 39-47.
- Palmer, M. A., Bernhardt, E. S., Schlesinger, W. H., Eshleman, K. N., Foufoula-Georgiou, E., Hendryx, M. S., ... & White, P. S. (2010). Mountaintop mining consequences. *Science*, 327(5962), 148-149.
- Paybins, K. S. (2003). Flow origin, drainage area, and hydrologic characteristics for headwater streams in the mountaintop coal-mining region of southern West Virginia, 2000–01. *Water Resources Investigations Report*, 02-4300.
- Pericak, A. A., Thomas, C. J., Kroodsma, D. A., Wasson, M. F., Ross, M. R., Clinton, N. E., ... & Amos, J. F. (2018). Mapping the yearly extent of surface coal mining in Central Appalachia using Landsat and Google Earth Engine. *PLoS one*, 13(7), e0197758.
- Pond, G. J., Passmore, M. E., Borsuk, F. A., Reynolds, L., & Rose, C. J. (2008). Downstream effects of mountaintop coal mining: comparing biological conditions using family- and genus-level macroinvertebrate bioassessment tools. *Journal of the North American Benthological Society*, 27(3), 717-737.
- Pond, G. J. (2010). Patterns of Ephemeroptera taxa loss in Appalachian headwater streams (Kentucky, USA). *Hydrobiologia*, 641(1), 185-201.
- Pond, G. J., Passmore, M. E., Pointon, N. D., Felbinger, J. K., Walker, C. A., Krock, K. J., ... & Nash, W. L. (2014). Long-term impacts on macroinvertebrates downstream of reclaimed

- mountaintop mining valley fills in central Appalachia. *Environmental Management*, 54(4), 919-933.
- R Core Team (2018). R: A language and environment for statistical computing. R Foundation for Statistical Computing. Vienna, Austria. URL <https://www.R-project.org/>.
- Sen, P. K. (1968). Estimates of the regression coefficient based on Kendall's tau. *Journal of the American Statistical Association*, 63(324), 1379-1389.
- Stoddard, J.L., Jeffries, D.S., Lükewille, A., Clair, T.A., Dillon, P.J., Driscoll, C.T., Forsius, M., Johannessen, M., Kahl, J.S., Kellogg, J.H. and Kemp, A., 1999. Regional trends in aquatic recovery from acidification in North America and Europe. *Nature*, 401(6753), p.575.
- Szöcs, E., Coring, E., Bäche, J., & Schäfer, R. B. (2014). Effects of anthropogenic salinization on biological traits and community composition of stream macroinvertebrates. *Science of the Total Environment*, 468, 943-949.
- Temnerud, J., & Bishop, K. 2005. Spatial variation of streamwater chemistry in two Swedish boreal catchments: Implications for environmental assessment. *Environmental Science & Technology*, 39(6), 1463-1469.
- Theil, H., 1950. A rank-invariant method of linear and polynomial regression analysis, 1, 2, and 3: *Ned. Akad. Wentsch Proc.*, 53, 386-392, 521-525, and 1397-1412.
- Timpano, A. J., Schoenholtz, S. H., Soucek, D. J., & Zipper, C. E. (2015). Salinity as a limiting factor for biological condition in Mining-Influenced central Appalachian headwater streams. *Journal of the American Water Resources Association*, 51(1), 240-250.
- Timpano, A. J., Vander Vorste, R., Soucek, D. J., Whitmore, K., Zipper, C. E., & Schoenholtz, S. H. (2017). Stream ecosystem response to mining-induced salinization in central Appalachia. *Final report to the Office of Surface Mining Reclamation and Enforcement (OSMRE Cooperative Agreement S15AC20028)*. Virginia Water Resources Research Institute.
- Timpano, A. J., Zipper, C. E., Soucek, D. J., & Schoenholtz, S. H. (2018a). Seasonal pattern of anthropogenic salinization in temperate forested headwater streams. *Water Research*, 133, 8-18.
- Timpano, A. J., Schoenholtz, S. H., Soucek, D. J., & Zipper, C. E. (2018b). Benthic macroinvertebrate community response to salinization in headwater streams in Appalachia USA over multiple years. *Ecological Indicators*, 91, 645-656.
- Tiwari, T., Buffam, I., Sponseller, R. A., & Laudon, H. (2017). Inferring scale-dependent processes influencing stream water biogeochemistry from headwater to sea. *Limnology and Oceanography*, 62(S1), S58-S70.
- USEPA. (1971). Method 160.1: residue, filterable (gravimetric, dried at 180 °C). Methods for the chemical analysis of water and wastes (MCAWW) (EPA/600/4-79/020)

- USEPA. (1996). U. S. *Method 1669: Sampling Ambient Water for Trace Metals at EPA Water Quality Criteria Levels*. EPA-821-R-96-011.
- USEPA. (2011a). The Effects of Mountaintop Mines and Valley Fills on Aquatic Ecosystems of the Central Appalachian Coalfields. Office of Research and Development, National Center for Environmental Assessment, Washington, DC. EPA/600/R-09/138F
- USEPA. (2011b). A field-based aquatic life benchmark for conductivity in central Appalachian streams. Washington, DC: U.S. Environmental Protection Agency, NCEA; 2011. EPA/600/R-10/023A. Available from: <http://cfpub.epa.gov/ncea/cfm/recordisplay.cfm?deid=233809>.
- USEPA. (2016). Aquatic Life Ambient Water Quality Criterion for Selenium – Freshwater. <https://www.epa.gov/wqc/aquatic-life-criterion-selenium>
- Wallace, J. B., & Webster, J. R. (1996). The role of macroinvertebrates in stream ecosystem function. *Annual Review of Entomology*, 41(1), 115-139.
- Whitmore, K. M., Schoenholtz, S. H., Soucek, D. J., Hopkins, W. A., & Zipper, C. E. (2018). Selenium dynamics in headwater streams of the central Appalachian coalfield. *Environmental Toxicology and Chemistry*, 37(10), 2714-2726.
- Zimmer, M. A., Bailey, S. W., McGuire, K. J., & Bullen, T. D. (2013). Fine scale variations of surface water chemistry in an ephemeral to perennial drainage network. *Hydrological Processes*, 27(24), 3438-3451.
- Zipper, C. E., Donovan, P. F., Jones, J. W., Li, J., Price, J. E., & Stewart, R. E. (2016). Spatial and temporal relationships among watershed mining, water quality, and freshwater mussel status in an eastern USA river. *Science of the Total Environment*, 541, 603-615.

APPENDIX A - GRAPHS OF CONTINUOUS SC DURING THE STUDY PERIOD (2011-2019)

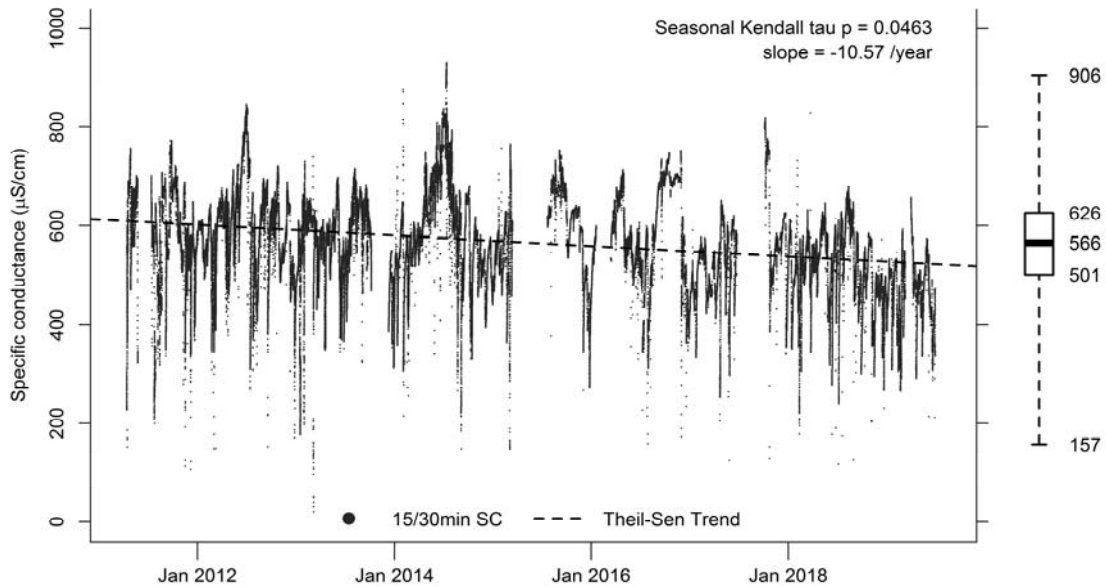


Figure A-1: Continuous (15/30-min interval) specific conductance (SC) for Birchfield creek (BIR, test stream). Seasonal Kendall tau P-value and Theil-Sen trend (dashed line) if statistically significant ($P < 0.05$). Boxplot of 15/30 minute continuous SC showing interquartile range, extreme values, and median.

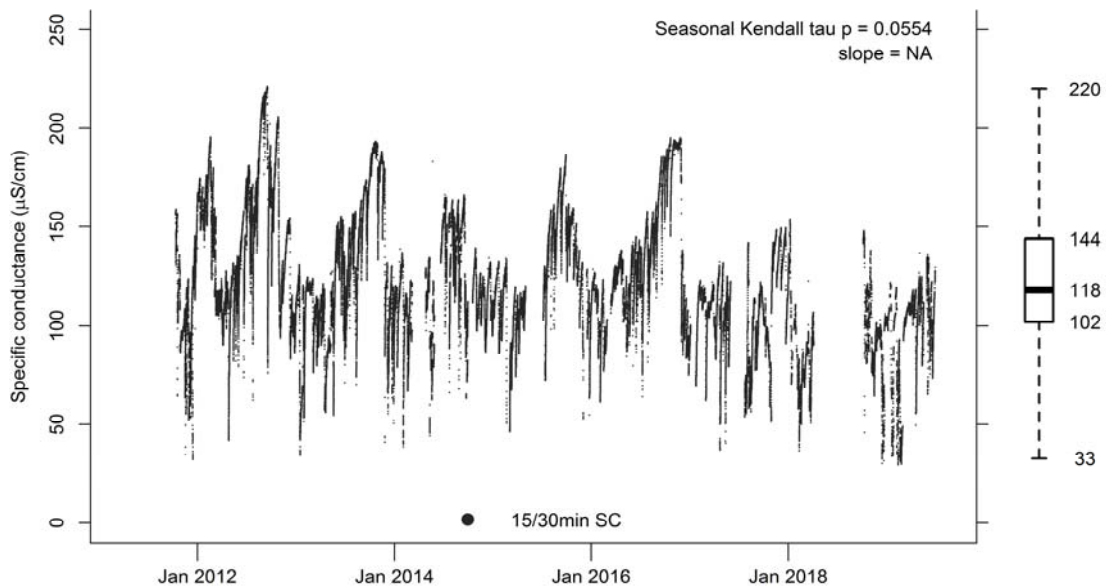


Figure A-2: Continuous (15/30-min interval) specific conductance (SC) for Copperhead Branch (COP, reference stream). Boxplot of 15/30 minute continuous SC showing interquartile range, extreme values, and median.

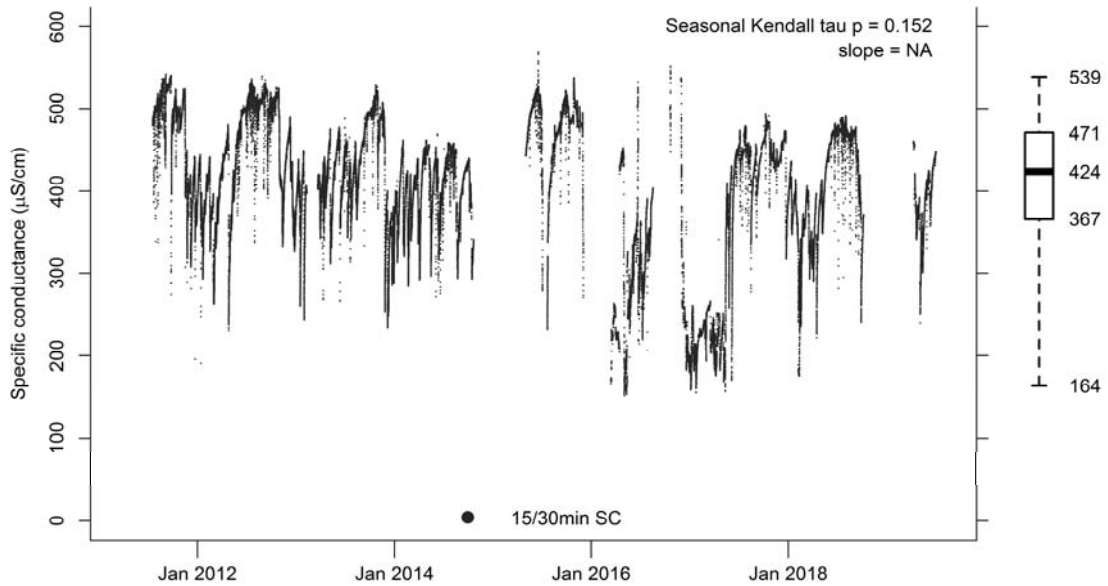


Figure A-3: Continuous (15/30-min interval) specific conductance (SC) for Crane Fork (CRA, test stream). Boxplot of 15/30 minute continuous SC showing interquartile range, extreme values, and median.

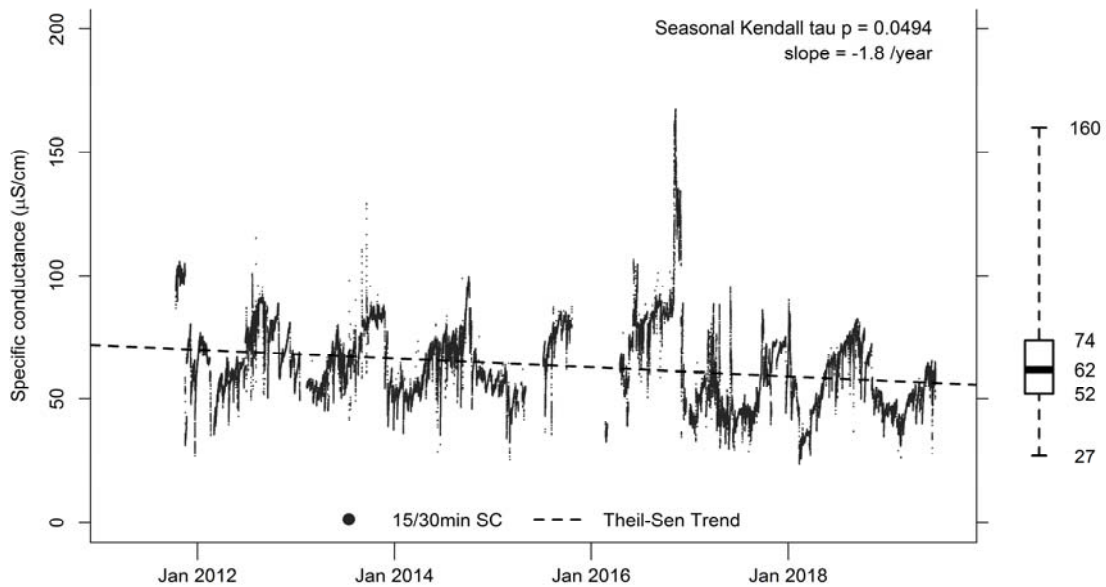


Figure A-4: Continuous (15/30-min interval) specific conductance (SC) for Crooked Branch (CRO, reference stream). Seasonal Kendall tau P-value and Theil-Sen trend (dashed line) if statistically significant ($P < 0.05$). Boxplot of 15/30 minute continuous SC showing interquartile range, extreme values, and median.

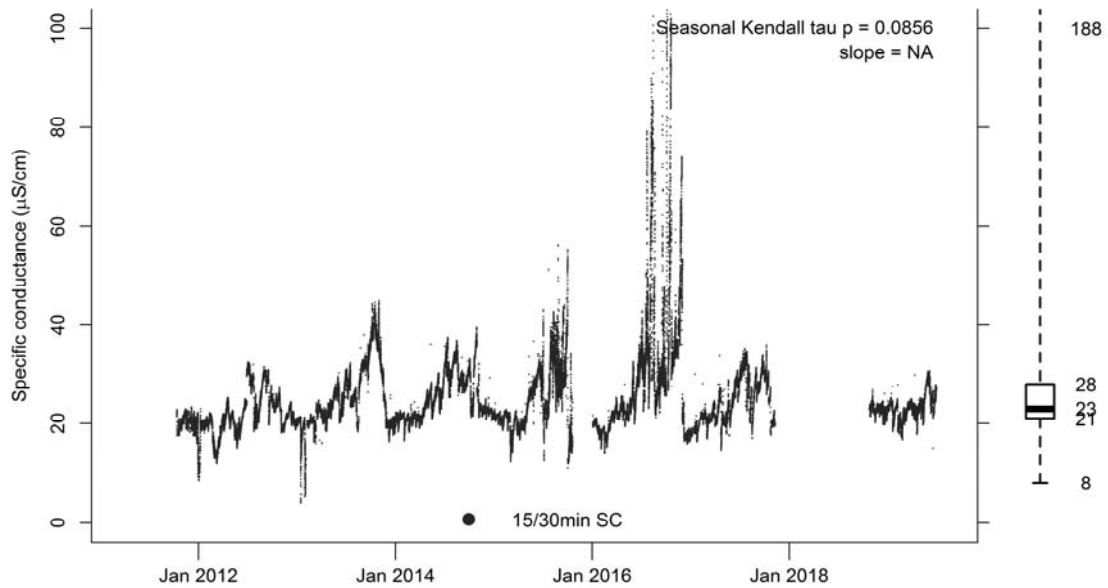


Figure A-5: Continuous (15/30-min interval) specific conductance (SC) for Eastland creek (EAS, reference stream). Boxplot of 15/30 minute continuous SC showing interquartile range, extreme values, and median.

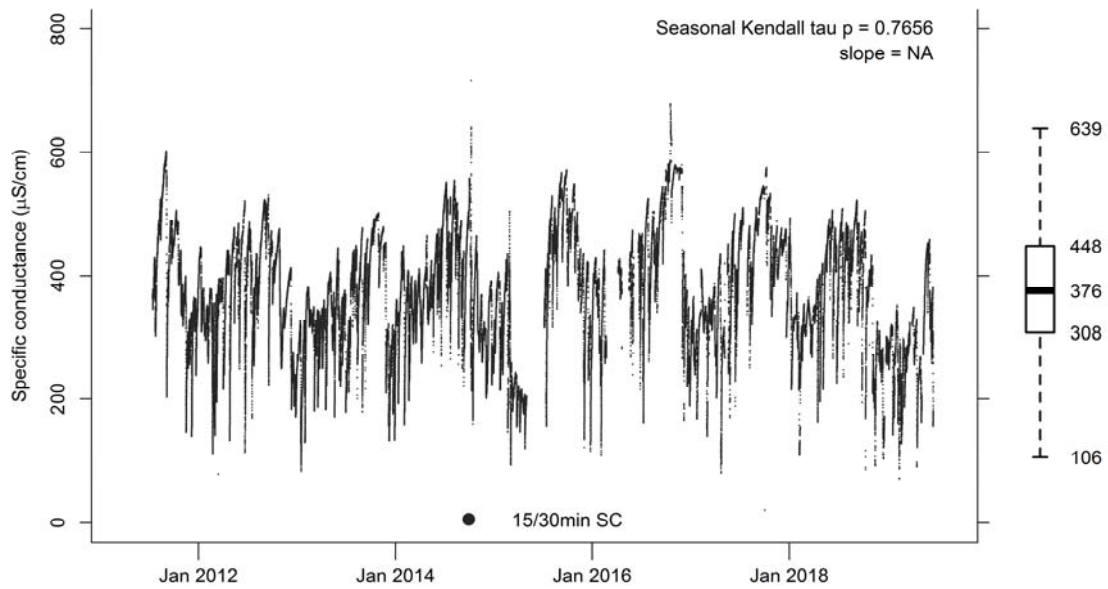


Figure A-6: Continuous (15/30-min interval) specific conductance (SC) for Fryingpan creek (FRY, test stream). Boxplot of 15/30 minute continuous SC showing interquartile range, extreme values, and median.

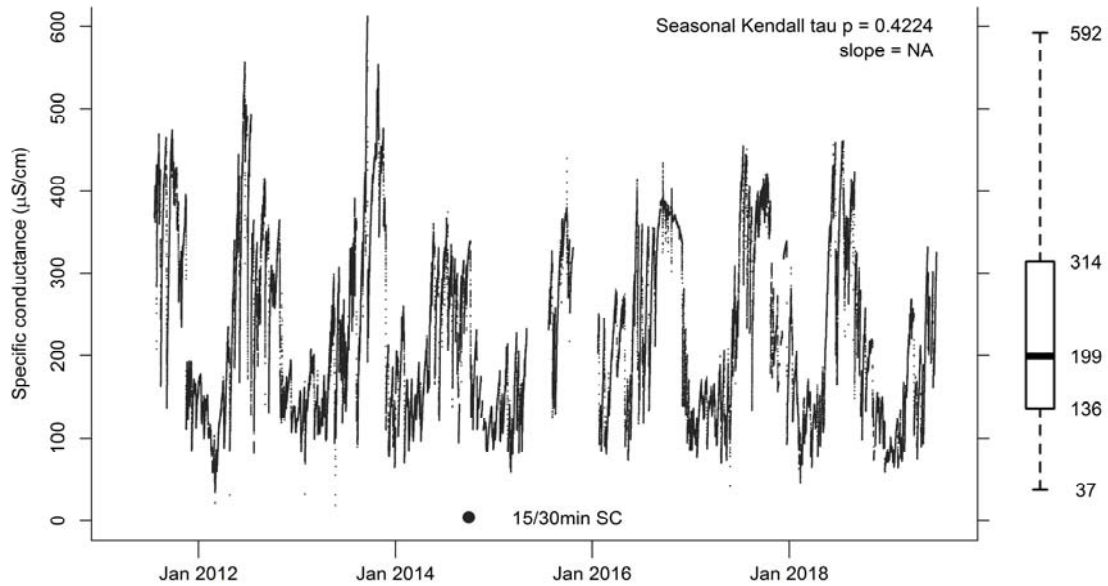


Figure A-7: Continuous (15/30-min interval) specific conductance (SC) for Grape Branch (GRA, test stream). Boxplot of 15/30 minute continuous SC showing interquartile range, extreme values, and median.

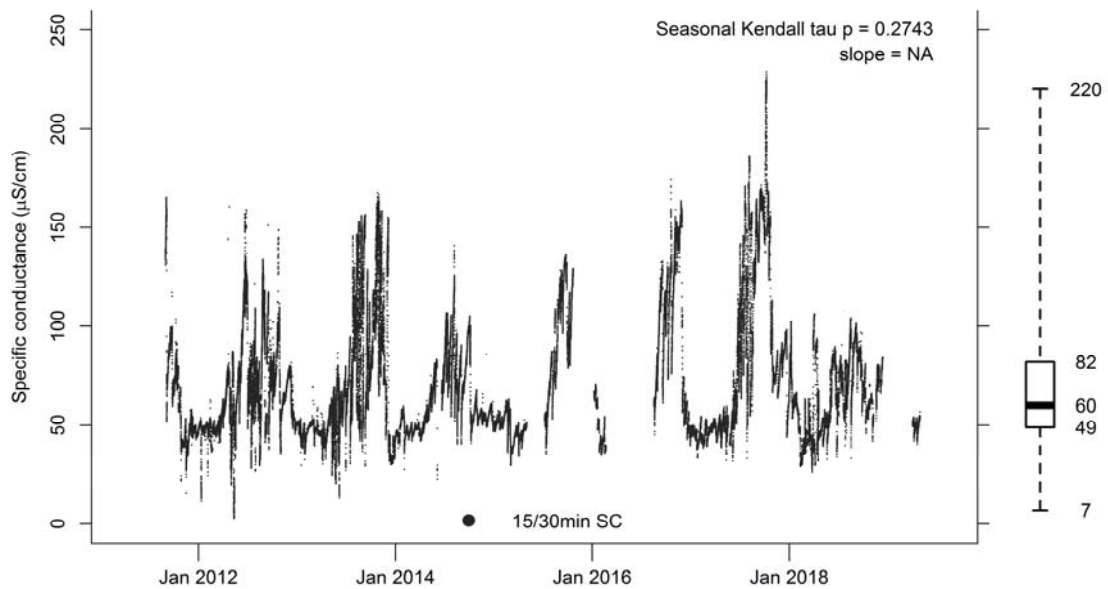


Figure A-8: Continuous (15/30-min interval) specific conductance (SC) for Hurricane Branch (HCN, reference stream). Boxplot of 15/30 minute continuous SC showing interquartile range, extreme values, and median.

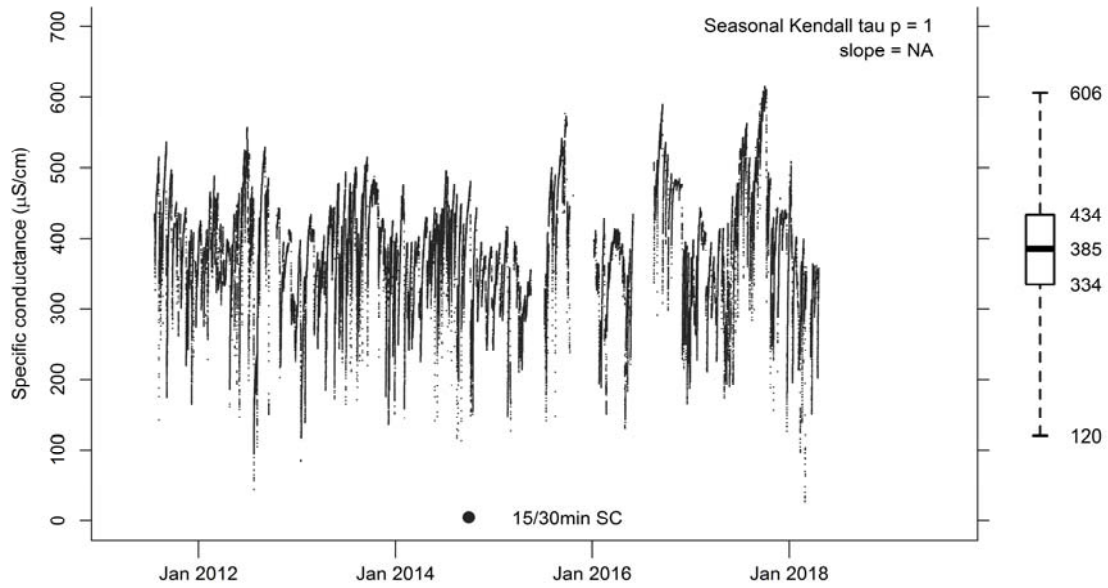


Figure A-9: Continuous (15/30-min interval) specific conductance (SC) for Hurricane Fork (HUR, test stream). Boxplot of 15/30 minute continuous SC showing interquartile range, extreme values, and median.

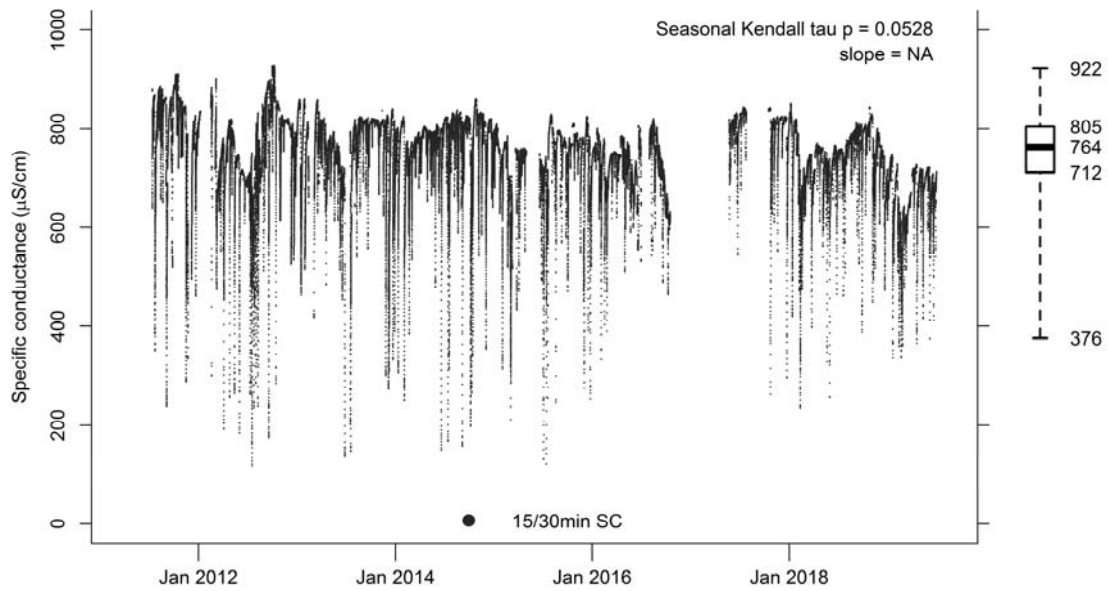


Figure A-10: Continuous (15/30-min interval) specific conductance (SC) for Kelly Branch (KEL, test stream). Boxplot of 15/30 minute continuous SC showing interquartile range, extreme values, and median.

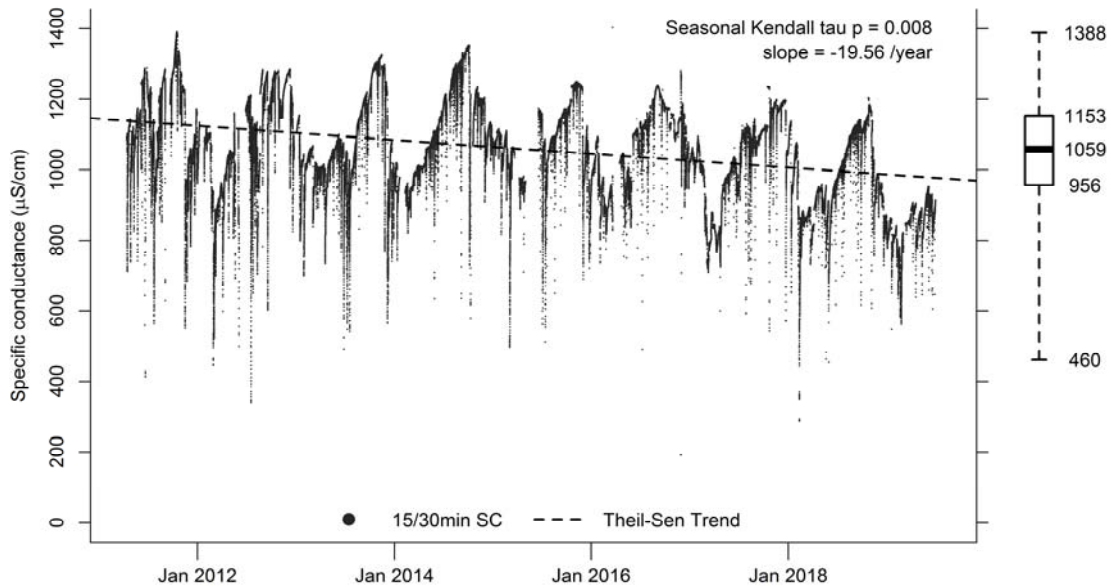


Figure A-11: Continuous (15/30-min interval) specific conductance (SC) for Kelly Branch Unnamed Tributary (KUT, test stream). Seasonal Kendall tau P-value and Theil-Sen trend (dashed line) if statistically significant ($P < 0.05$). Boxplot of 15/30 minute continuous SC showing interquartile range, extreme values, and median

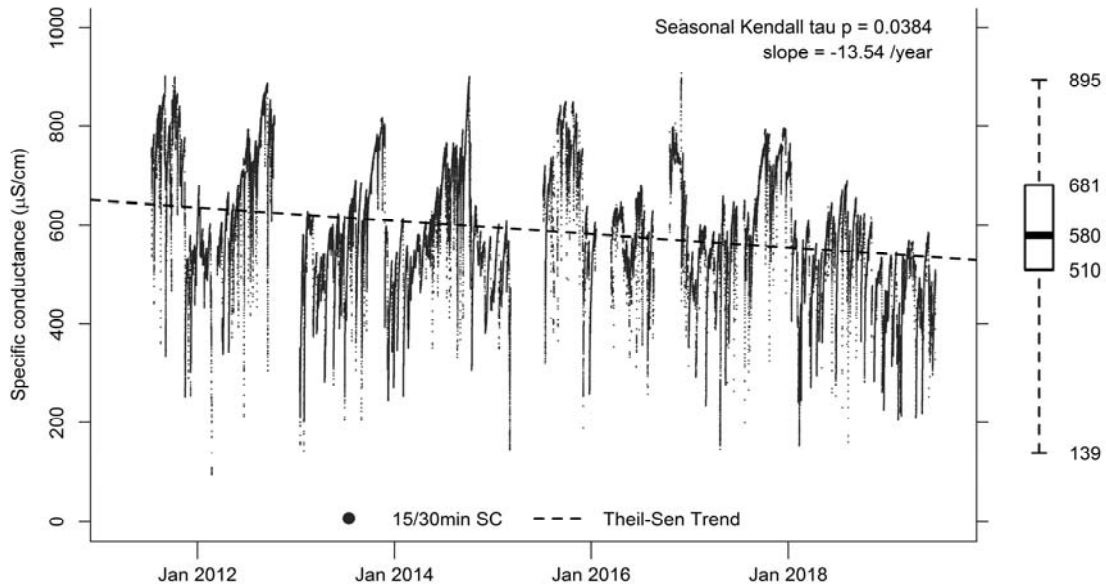


Figure A-12: Continuous (15/30-min interval) specific conductance (SC) for Laurel Branch (LAB, test stream). Seasonal Kendall tau P-value and Theil-Sen trend (dashed line) if statistically significant ($P < 0.05$). Boxplot of 15/30 minute continuous SC showing interquartile range, extreme values, and median.

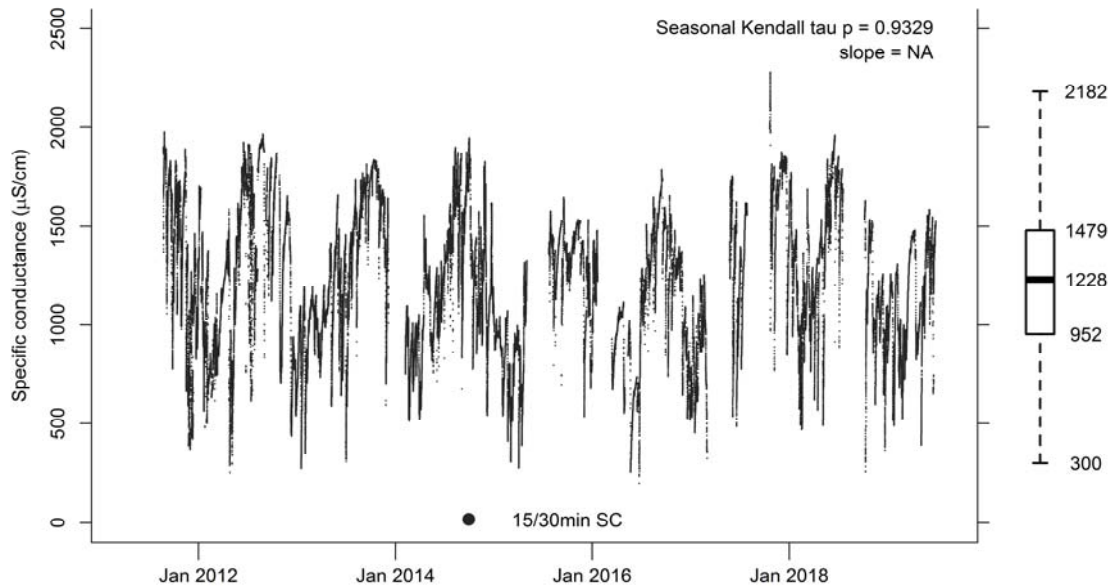


Figure A-13: Continuous (15/30-min interval) specific conductance (SC) for Left Fork of Long Fork of Coal Fork (LLC, test stream). Boxplot of 15/30 minute continuous SC showing interquartile range, extreme values, and median

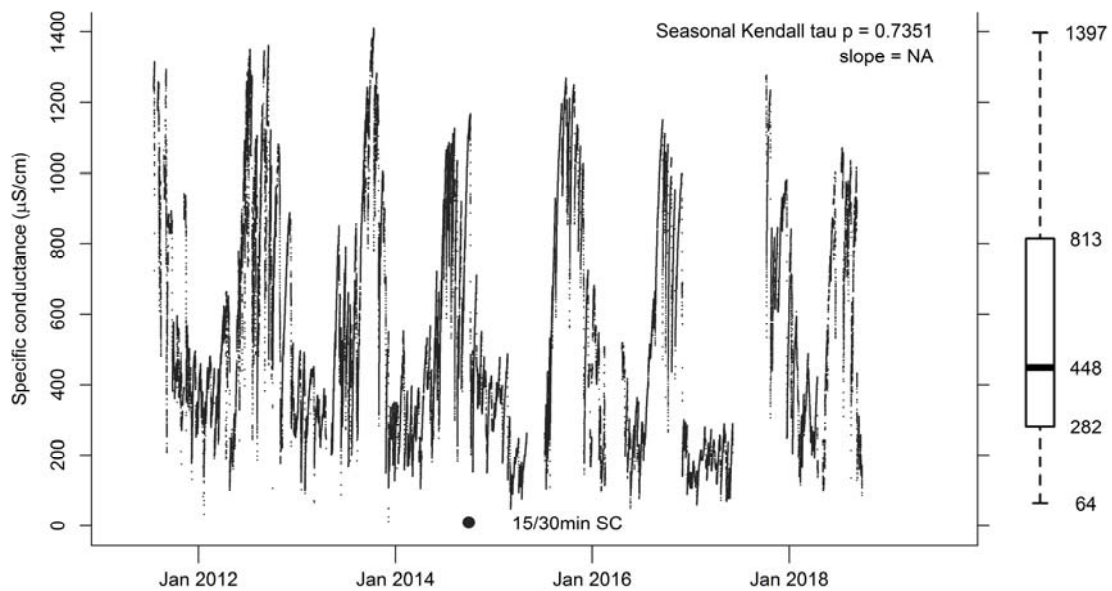


Figure A-14: Continuous (15/30-min interval) specific conductance (SC) for Longlick Branch East Fork (LLE, test stream). Boxplot of 15/30 minute continuous SC showing interquartile range, extreme values, and median

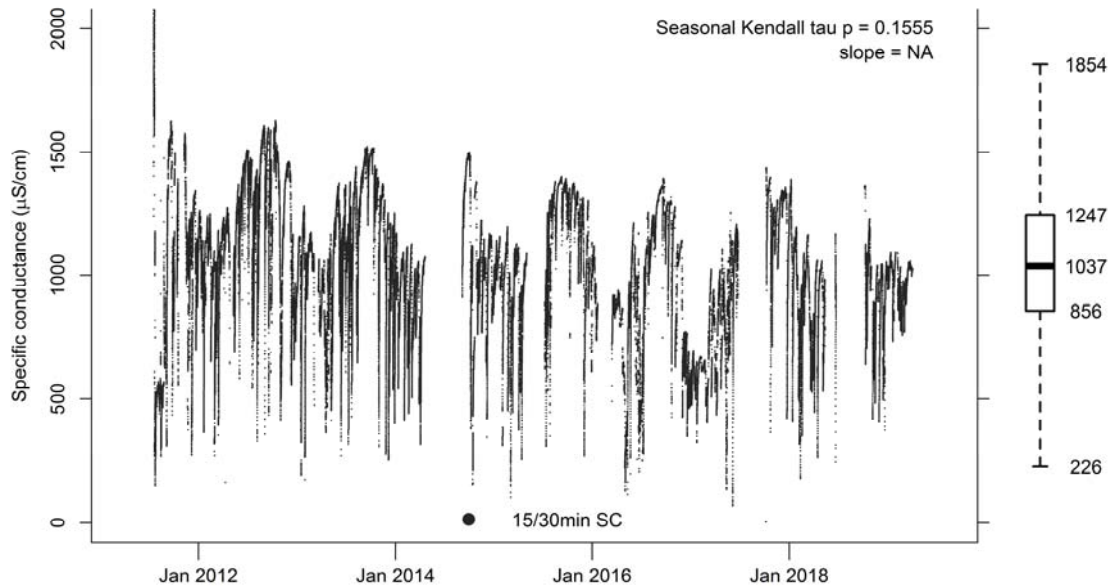


Figure A-15: Continuous (15/30-min interval) specific conductance (SC) for Longlick Branch West Fork (LLW, test stream). Boxplot of 15/30 minute continuous SC showing interquartile range, extreme values, and median.

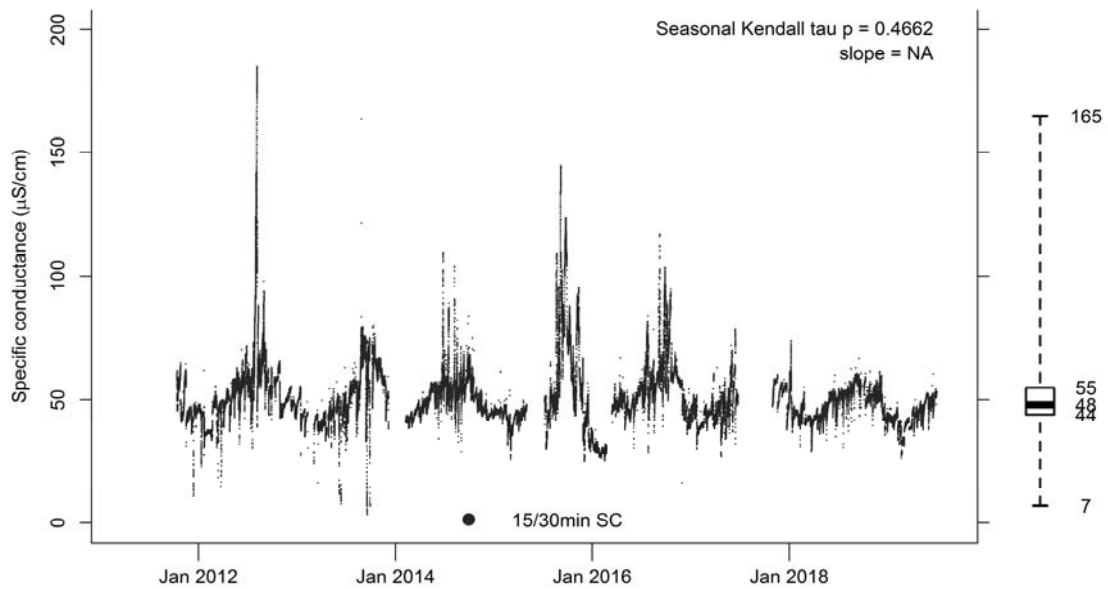


Figure A-16: Continuous (15/30-min interval) specific conductance (SC) for Middle Camp Branch (MCB, reference stream). Boxplot of 15/30 minute continuous SC showing interquartile range, extreme values, and median.

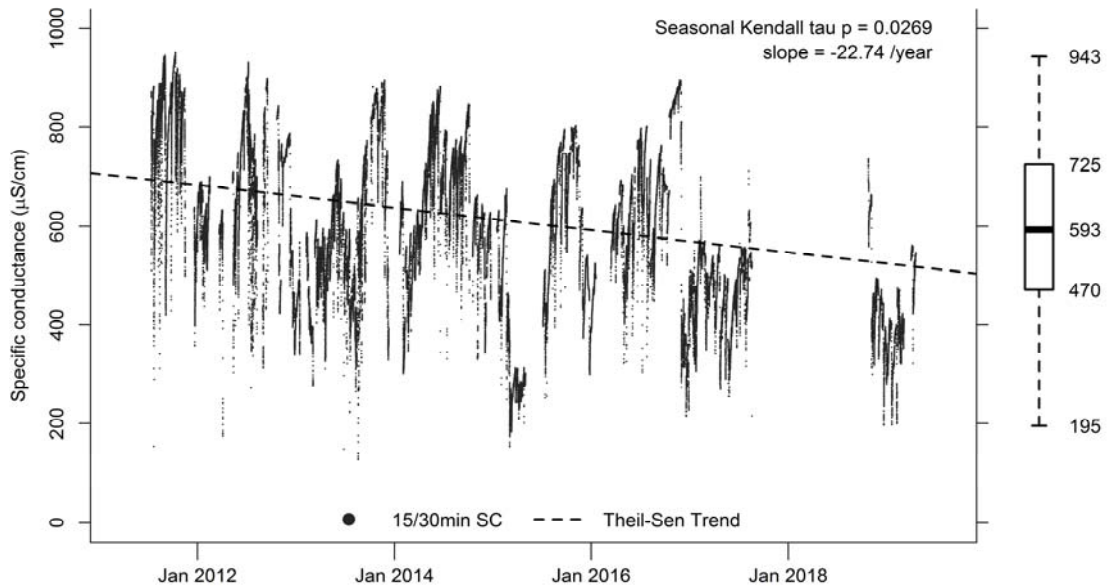


Figure A-17: Continuous (15/30-min interval) specific conductance (SC) for Mill Branch West Fork (MIL, test stream). Seasonal Kendall tau P-value and Theil-Sen trend (dashed line) if statistically significant ($P < 0.05$). Boxplot of 15/30 minute continuous SC showing interquartile range, extreme values, and median.

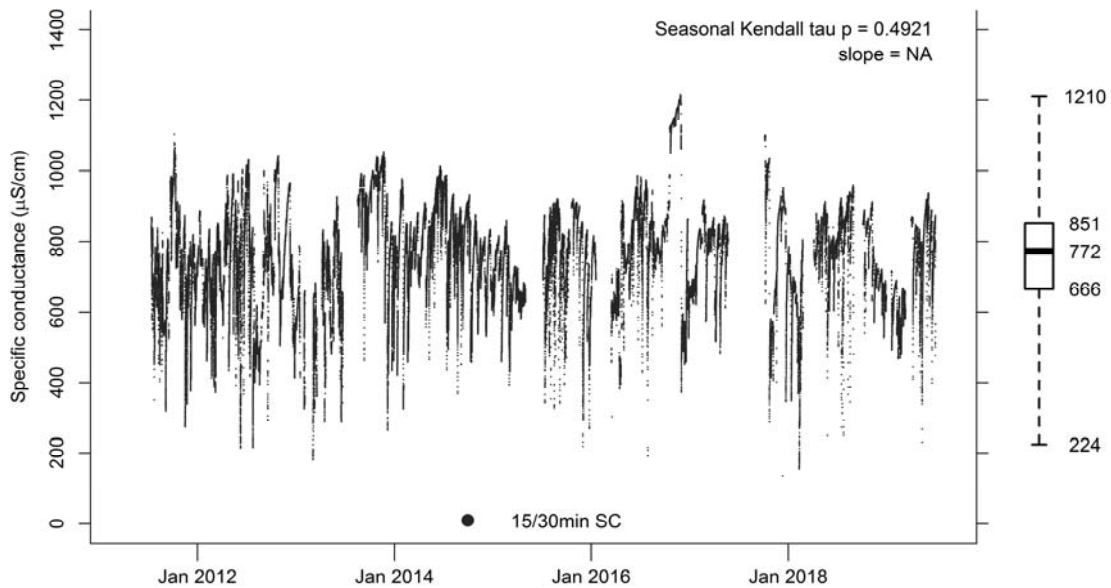


Figure A-18: Continuous (15/30-min interval) specific conductance (SC) for Powell River (POW, test stream). Boxplot of 15/30 minute continuous SC showing interquartile range, extreme values, and median.

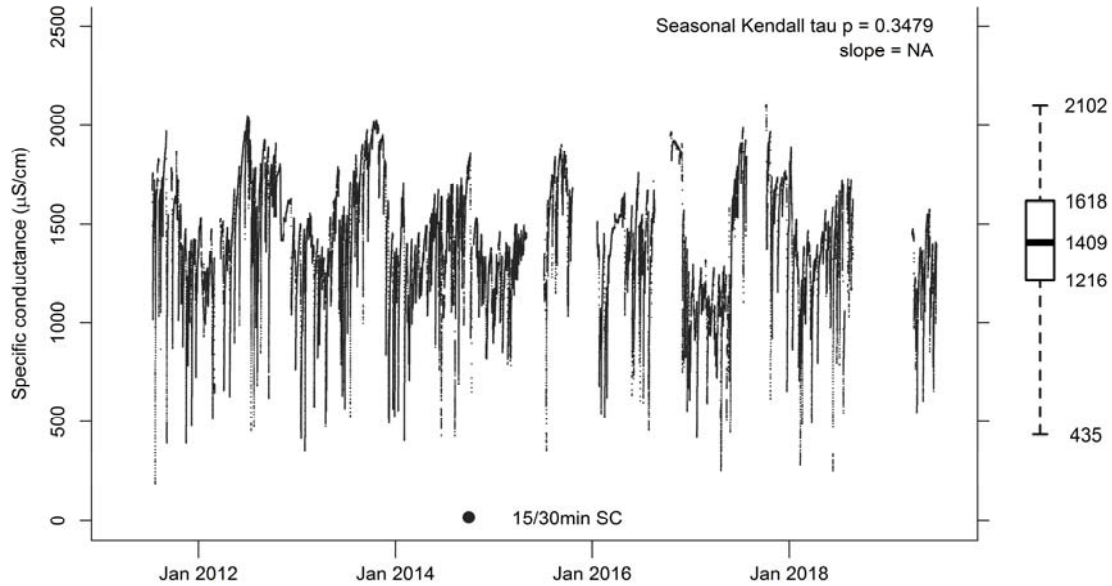


Figure A-19: Continuous (15/30-min interval) specific conductance (SC) for Rickey Branch (RIC, test stream). Boxplot of 15/30 minute continuous SC showing interquartile range, extreme values, and median.

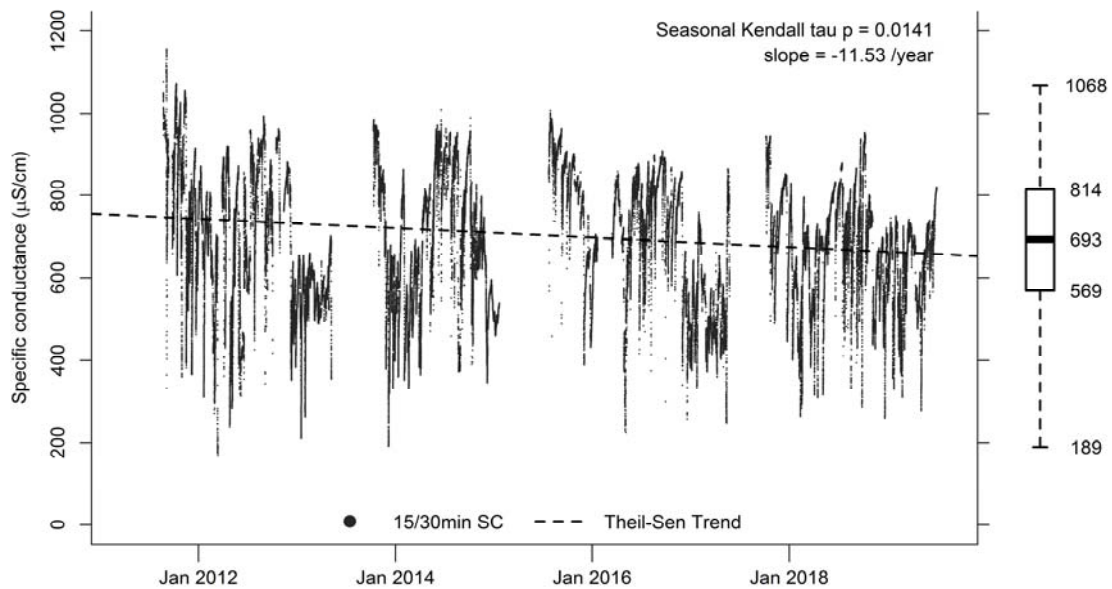


Figure A-20: Continuous (15/30-min interval) specific conductance (SC) for Rockhouse Fork (ROC, test stream). Seasonal Kendall tau P-value and Theil-Sen trend (dashed line) if statistically significant ($P < 0.05$). Boxplot of 15/30 minute continuous SC showing interquartile range, extreme values, and median.

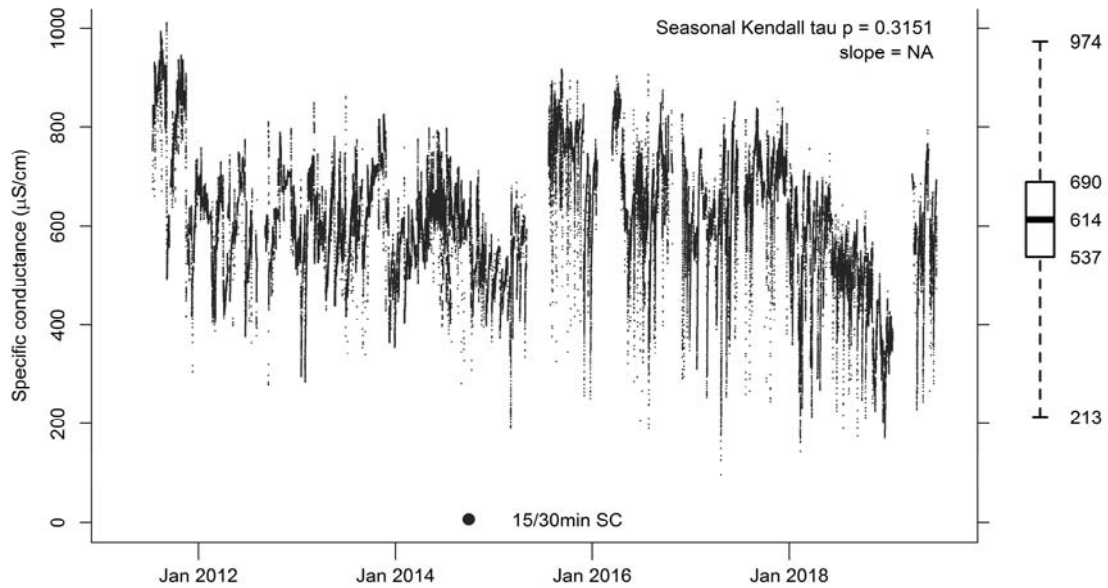


Figure A-191: Continuous (15/30-min interval) specific conductance (SC) for Roll Pone Branch (ROL, test stream). Boxplot of 15/30 minute continuous SC showing interquartile range, extreme values, and median.

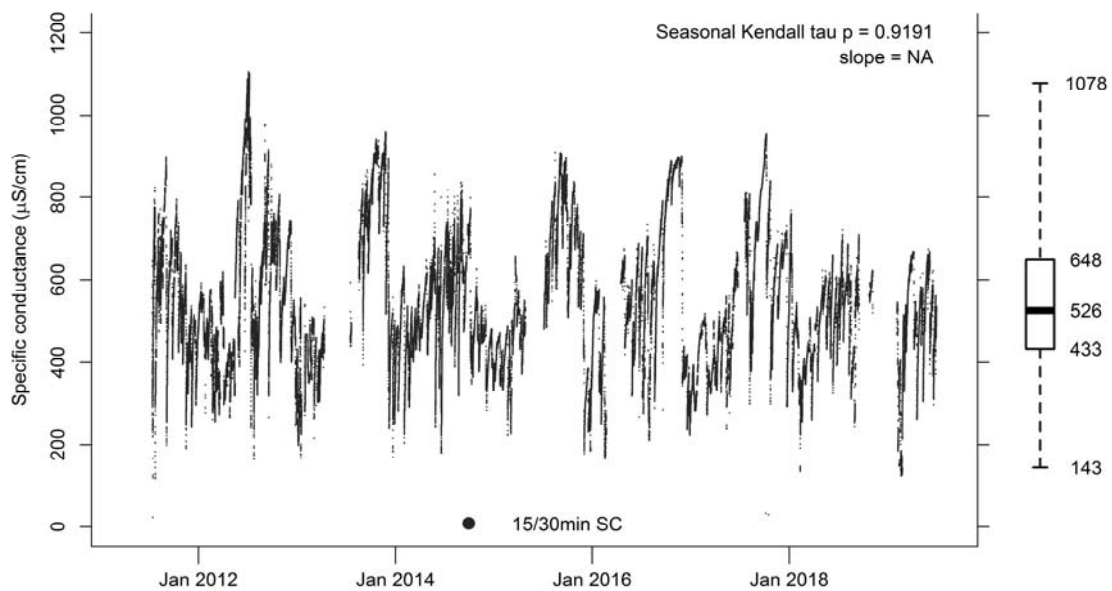


Figure A-22: Continuous (15/30-min interval) specific conductance (SC) for Rickey Branch Unnamed Tributary (RUT, test stream). Boxplot of 15/30 minute continuous SC showing interquartile range, extreme values, and median.

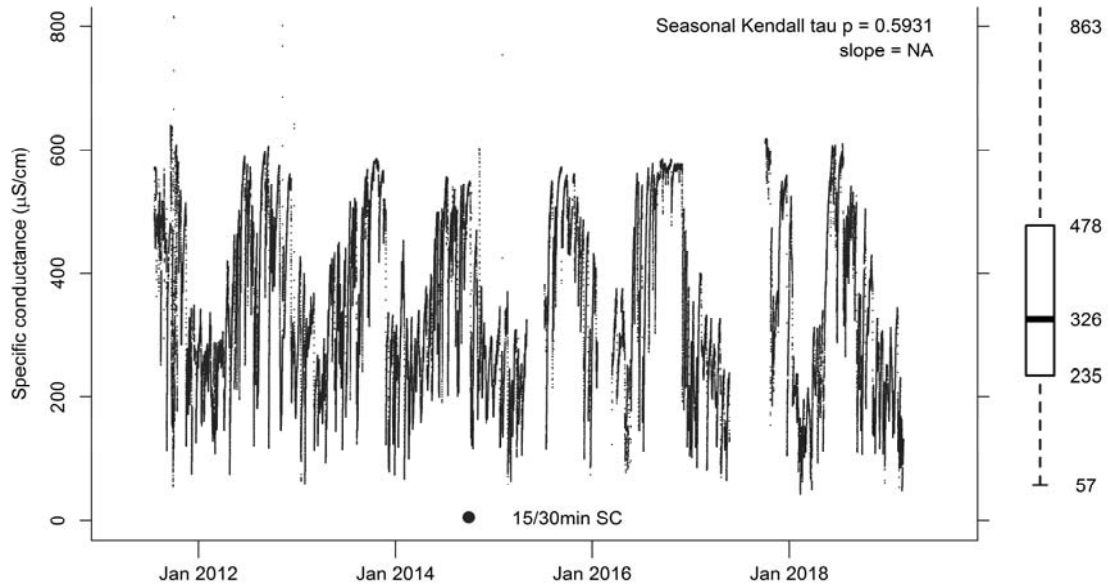


Figure A-203: Continuous (15/30-min interval) specific conductance (SC) for Spruce Pine Creek (SPC, test stream). Boxplot of 15/30 minute continuous SC showing interquartile range, extreme values, and median.

APPENDIX B - SUMMARY OF TEMPORAL TRENDS IN SPECIFIC CONDUCTANCE, ION MATRIX, AND BENTHIC MACROINVERTEBRATES COMMUNITY METRICS

Table B-1: Summary table of temporal trends in specific conductance (SC), ion matrix, and biological community metrics

| Site | Site type | Mean SC | SC trend | SC slope | Tau | Richness | EPT richness | E richness | % Ephemeroptera | scraper richness | shannon diversity | ephemeroptera richness less Beatidae | %ephemeroptera less Beatidae | SO4 : HCO3 | Ca : Mg | %mined 1980-2011 | additional %mined 2011-2016 |
|------|-----------|---------|----------|----------|-------|----------|--------------|------------|-----------------|------------------|-------------------|--------------------------------------|------------------------------|------------|---------|------------------|-----------------------------|
| EAS | Ref | 25 | | | 0.21 | | | | | | | | | | Neg | 0 | 0 |
| MCB | Ref | 51 | | | -0.07 | | | | | Neg | | | | | Neg | 0 | 0 |
| CRO | Ref | 64 | Neg | -1.80 | -0.32 | Pos | | | | | | | | | | 0 | 0 |
| HCN | Ref | 68 | | | 0.07 | | | | | | | | | | | 0 | 0 |
| COP | Ref | 125 | | | -0.31 | | | | | | | | | | | 0 | 0 |
| GRA | Test | 226 | | | -0.07 | | | | | | | | | | | 2.1 | 0 |
| SPC | Test | 349 | | | -0.05 | Pos | | | | | | | | | | 3.8 | 0 |
| FRY | Test | 371 | | | -0.03 | | | | | | | | | | | 4.5 | 0.8 |
| HUR | Test | 383 | | | -0.01 | | | | | Pos | | | | Neg | | 20.7 | 0 |
| CRA | Test | 416 | | | -0.26 | | | | | | | | | | | 0 | 0 |
| RUT | Test | 554 | | | 0.00 | | | | Neg | | | | | Neg | Neg | 10.2 | 0 |
| LLE | Test | 562 | | | -0.10 | | Pos | Pos | | Pos | | Pos | | Neg | | 10.9 | 0 |
| BIR | Test | 571 | Neg | -10.57 | -0.24 | | | | | | | | | | | 5.4 | 0 |
| LAB | Test | 599 | Neg | -13.54 | -0.28 | Pos | | | | Pos | | | | Neg | | 7.6 | 0 |
| MIL | Test | 608 | Neg | -22.74 | -0.39 | | | | | | | | | Neg | Neg | 51.6 | 0.8 |
| ROL | Test | 618 | | | -0.15 | | | | | | | | | | | 29.9 | 0 |
| ROC | Test | 690 | Neg | -11.53 | -0.16 | | | | | Neg | | | | Neg | Neg | 30.4 | 0.5 |
| KEL | Test | 757 | | | -0.29 | | | | | Pos | | | | Neg | Neg | 56.3 | 2.4 |
| POW | Test | 761 | | | 0.06 | Pos | Pos | | | | Pos | Pos | | Neg | | 60.7 | 7.7 |
| LLW | Test | 1063 | | | -0.23 | Pos | Pos | | | | | | | Neg | | 26.4 | 0 |
| KUT | Test | 1068 | Neg | -19.56 | -0.40 | | | | | | | | | Neg | | 39.3 | 0.5 |
| LLC | Test | 1218 | | | -0.02 | | Neg | Neg | | | | | | | | 19.2 | 5.7 |
| RIC | Test | 1418 | | | -0.06 | | | | | | | | | Neg | Neg | 34.7 | 0 |

APPENDIX C - SPATIAL AND FLOW-DRIVEN DYNAMICS OF MAJOR IONS AND TRACE ELEMENTS

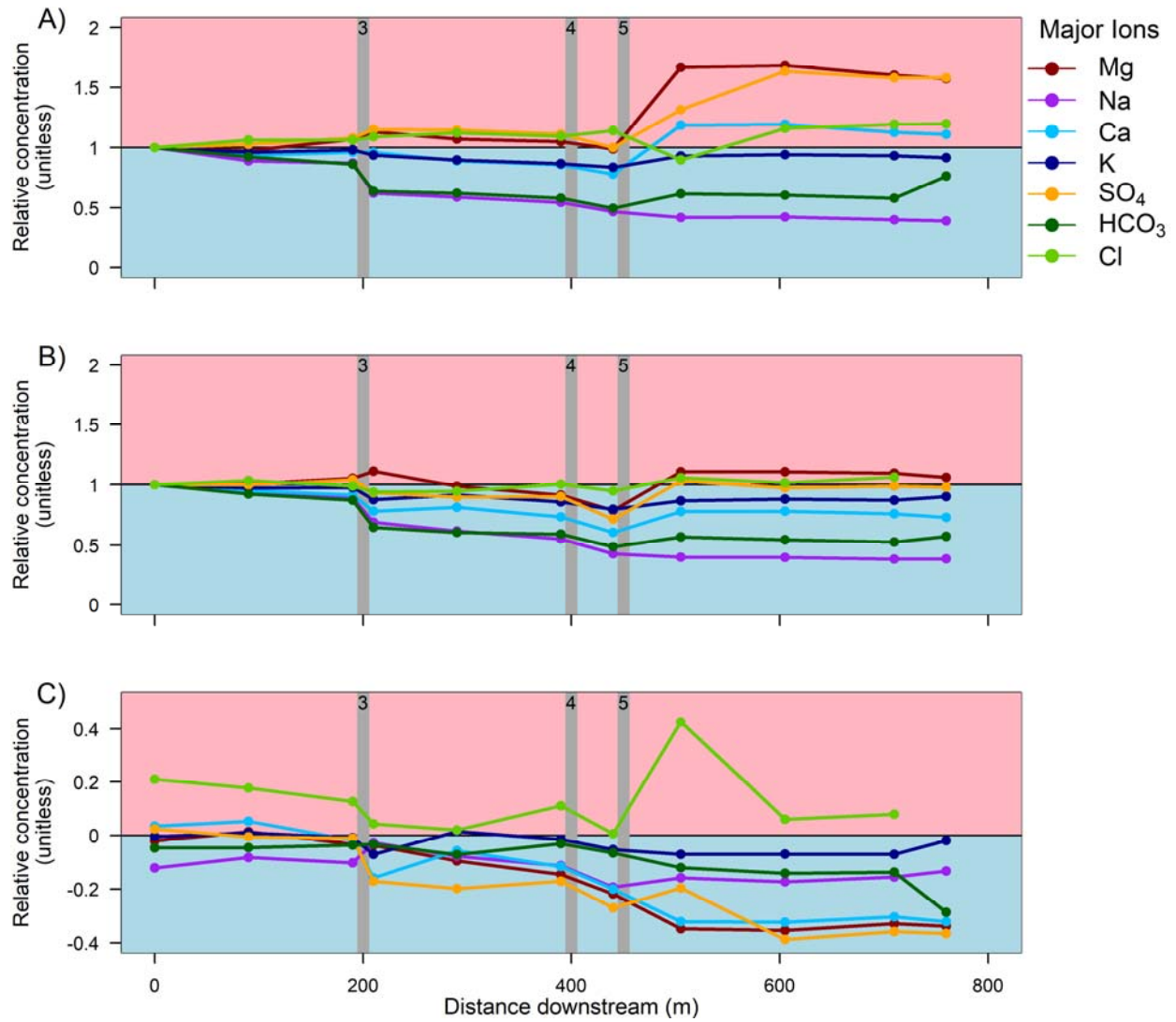


Figure C-1: Relative concentrations of major ions in Hurricane Branch, VA. A) Proportion of concentration at sampling location to concentration at origin under baseflow and B) highflow. C) Relative change in concentrations of major ions under highflow compared to baseflow. Shaded red areas symbolize enriched relative concentrations. Shaded blue areas symbolize diluted relative concentrations.

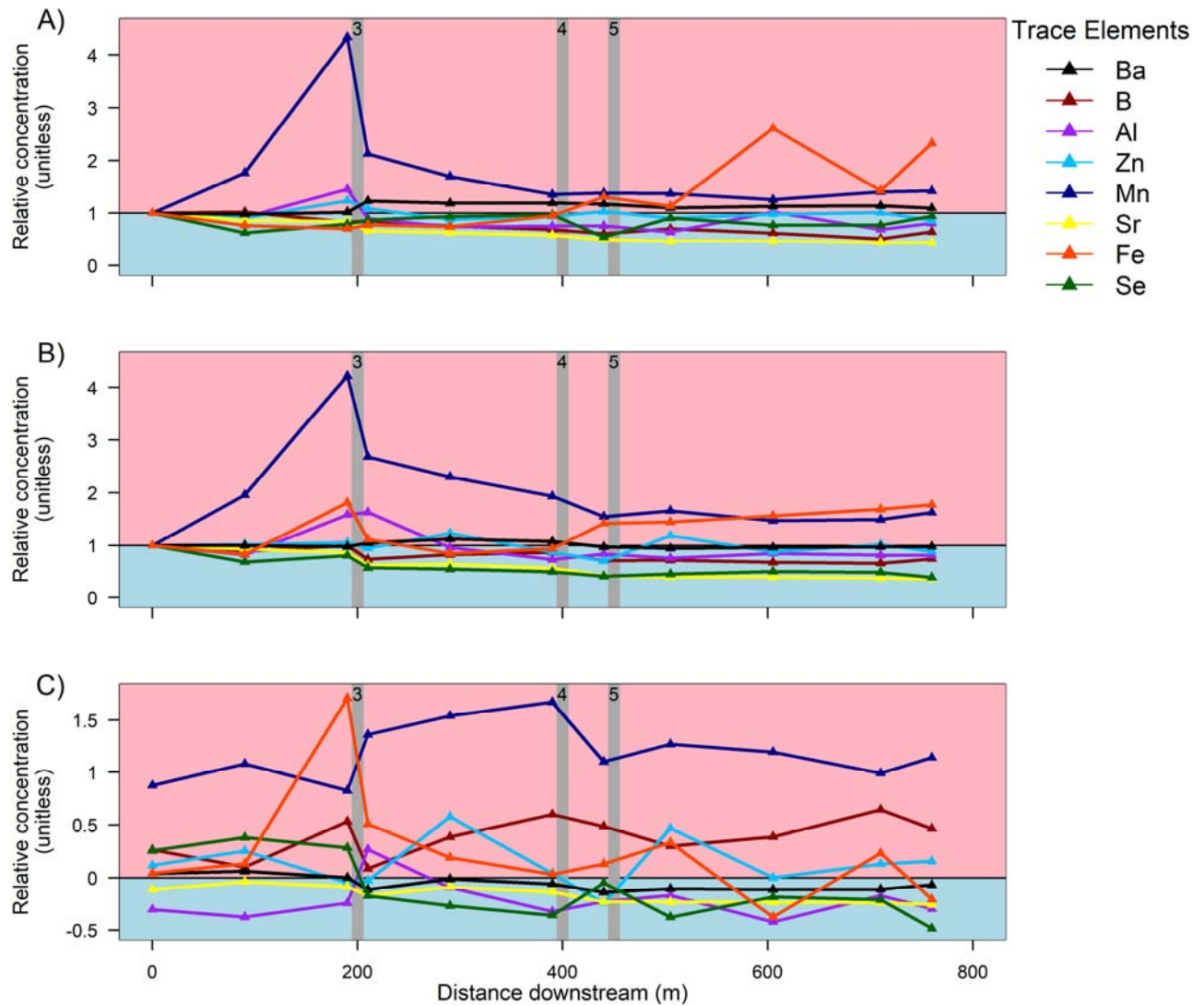


Figure C-2: Relative concentrations of trace elements in Hurricane Branch, VA. A) Proportion of concentration at sampling location to concentration at origin under baseflow and B) highflow. C) Relative change in concentrations of major ions under highflow compared to baseflow. Shaded red areas symbolize enriched relative concentrations. Shaded blue areas symbolize diluted relative concentrations.

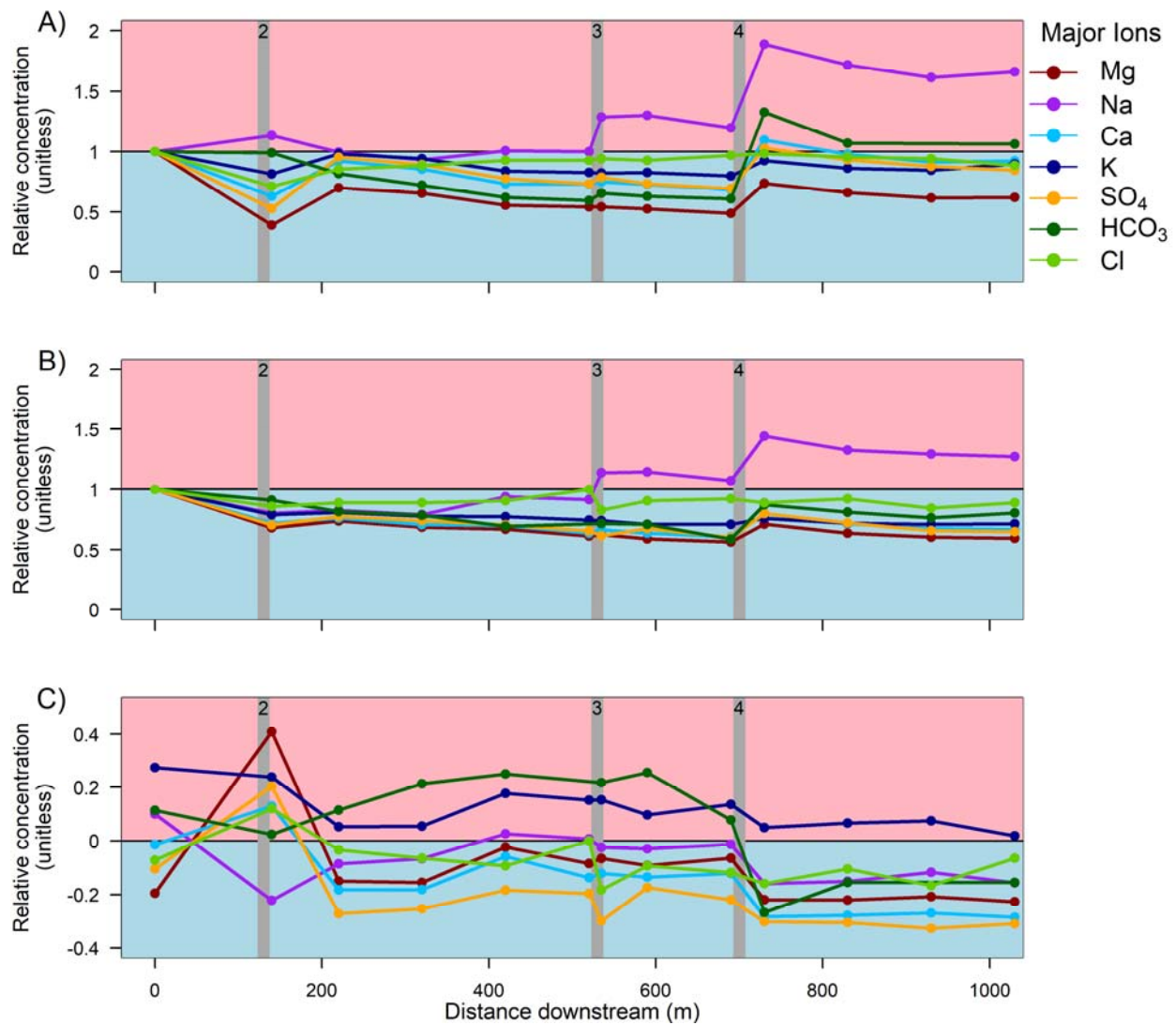


Figure C-3: Relative concentrations of major ions in Longlick Branch East Fork, WV. A) Proportion of concentration at sampling location to concentration at origin under baseflow and B) highflow. C) Relative change in concentrations of major ions under highflow compared to baseflow. Shaded red areas symbolize enriched relative concentrations. Shaded blue areas symbolize diluted relative concentrations.

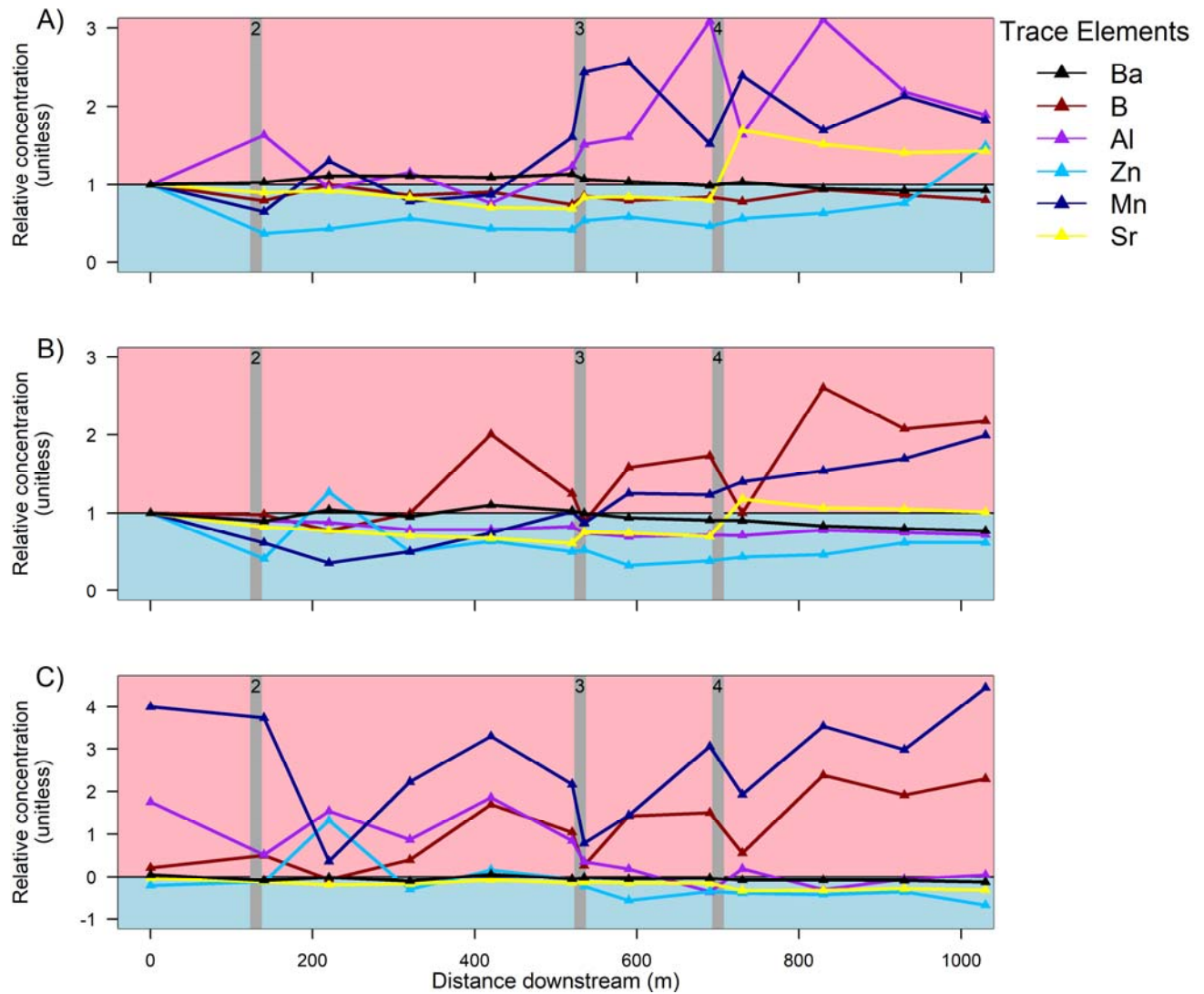


Figure C-4: Relative concentrations of trace elements in Longlick Branch East Fork, WV. A) Proportion of concentration at sampling location to concentration at origin under baseflow and B) highflow. C) Relative change in concentrations of major ions under highflow compared to baseflow. Shaded red areas symbolize enriched relative concentrations. Shaded blue areas symbolize diluted relative concentrations.

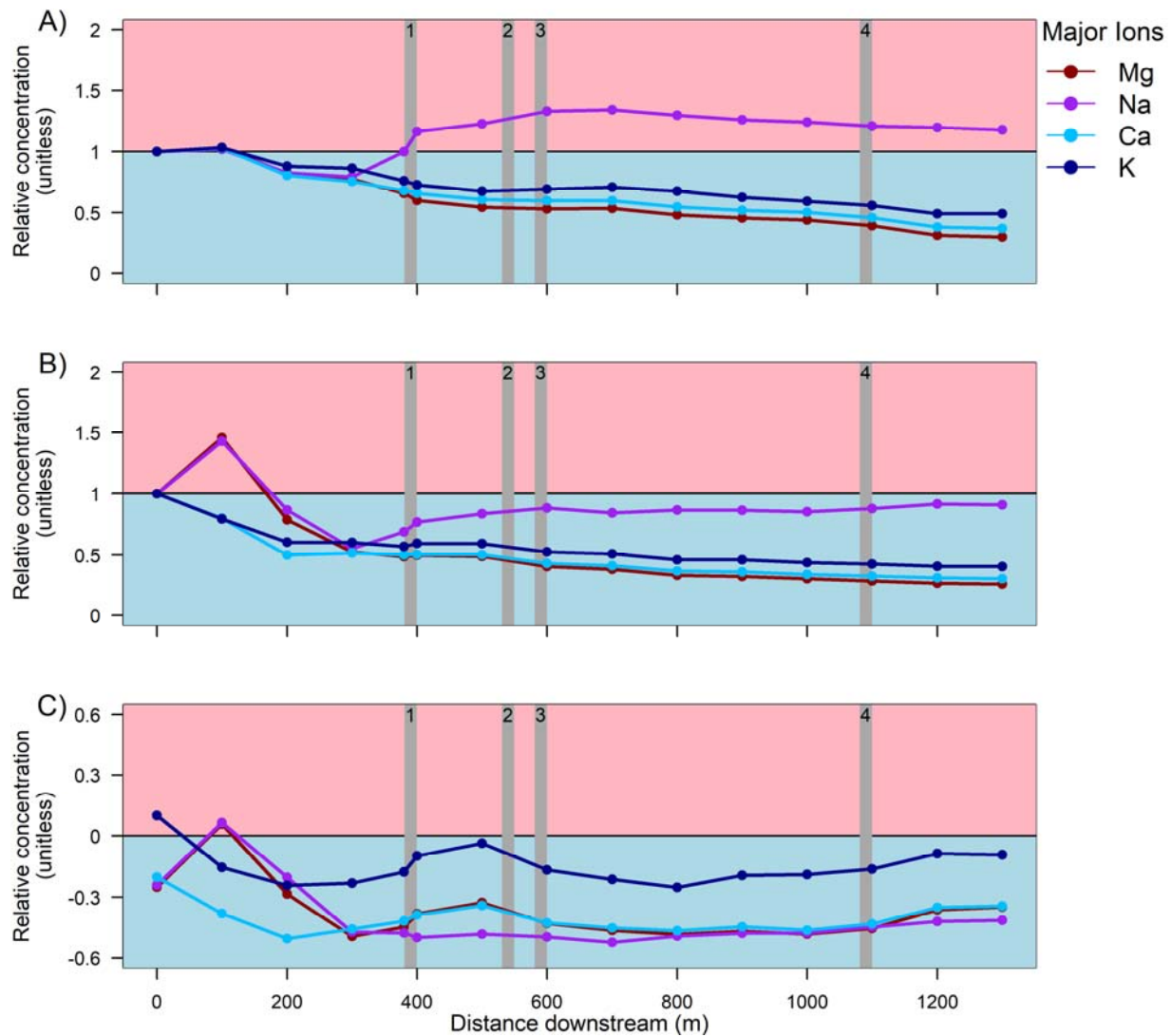


Figure C-5: Relative concentrations of major ions in Roll Pone Branch, VA. A) Proportion of concentration at sampling location to concentration at origin under baseflow and B) highflow. C) Relative change in concentrations of major ions under highflow compared to baseflow. Shaded red areas symbolize enriched relative concentrations. Shaded blue areas symbolize diluted relative concentrations.

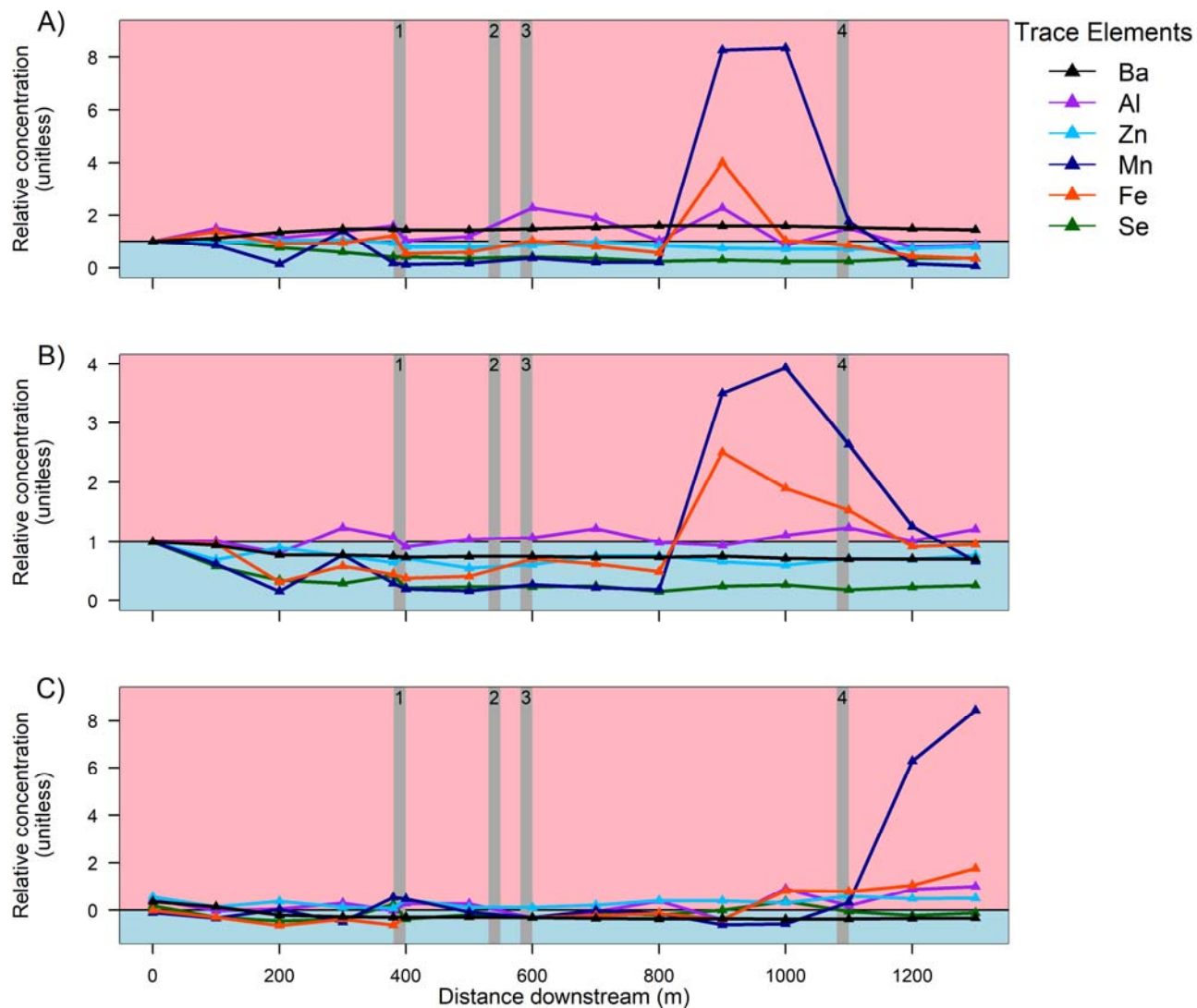


Figure C-6: Relative concentrations of trace elements in Roll Pone Branch, VA. A) Proportion of concentration at sampling location to concentration at origin under baseflow and B) highflow. C) Relative change in concentrations of major ions under highflow compared to baseflow. Shaded red areas symbolize enriched relative concentrations. Shaded blue areas symbolize diluted relative concentrations.

Table C-1: Concentrations of major ions and trace elements at the flow origin under baseflow and highflow conditions.

| Site Id | flow type | SC ¹ | Flow origin major ion and trace element concentrations (µg/L) | | | | | | | | | | | | | | |
|---------|-----------|-----------------|---|------|-----------------|-------|--------|------|--------|-------|-------|-------|-------------------|-------|-------------------|--------|-------|
| | | | HCO ₃ | Cl | SO ₄ | Na | Mg | K | Ca | B | Al | Mn | Fe | Zn | Se | Sr | Ba |
| HUR | high | 284 | 67.26 | 0.65 | 81.94 | 15.51 | 11.05 | 2.27 | 27.09 | 14.15 | 18.62 | 6.56 | 11.62 | 14.98 | 1.96 | 559.71 | 26.13 |
| HUR | base | 290 | 70.53 | 0.54 | 80.02 | 17.64 | 11.27 | 2.28 | 26.19 | 11.19 | 26.69 | 3.50 | 11.13 | 13.40 | 1.56 | 628.99 | 25.07 |
| LLE | high | 314 | 26.98 | 0.65 | 119.00 | 2.85 | 18.79 | 2.23 | 30.24 | 8.61 | 10.57 | 1.15 | <MRL ³ | 15.42 | <MRL ⁴ | 452.63 | 41.27 |
| LLE | base | 419 | 24.24 | 0.70 | 132.86 | 2.59 | 23.33 | 1.75 | 30.67 | 7.08 | 3.84 | 0.23 | <MRL | 19.51 | <MRL | 468.93 | 39.24 |
| ROL | high | 1111 | ND ² | ND | ND | 11.92 | 95.49 | 6.50 | 161.26 | ND | 4.63 | 15.57 | 10.84 | 16.93 | 2.03 | ND | 50.65 |
| ROL | base | 1741 | ND | ND | ND | 15.70 | 127.40 | 5.90 | 202.10 | ND | 3.20 | 17.40 | 10.90 | 10.80 | 1.70 | ND | 37.20 |

¹SC- specific conductance (µs/cm). ²ND- no data collected. ³Iron (Fe) MRL – 10.0 µg/L. ⁴Selenium (Se) MRL – 0.5 µg/L.